X-731-70-51

NASA TM X-63828

L-BAND PERFORMANCE CHARACTERISTICS OF THE ATS 5 SPACECRAFT

FREDRIC KISSEL

FEBRUARY 1970
REVISED
MAY 1970

GSFC

GODDARD SPACE FLIGHT CENTER
GREENBELT, MARYLAND

N70-30432

L-BAND PERFORMANCE CHARACTERISTICS OF THE ATS 5 SPACECRAFT

Fredric Kissel

Goddard Space Flight Center
Greenbelt, Maryland

February 1970
Revised May 1970

X-731-70-51

L-BAND PERFORMANCE CHARACTERISTICS OF THE ATS 5 SPACECRAFT

Fredric Kissel

February 1970

Revised

May 1970

GODDARD SPACE FLIGHT CENTER
Greenbelt, Maryland

X-731-70-51

L BAND PERFORMANCE CHARACTERISTICS

OF THE ATS-5 SPACECRAFT

Frederick J. Kissel

May 1970

GODDARD SPACE FLIGHT CENTER
Greenbelt, Maryland

TABLE OF CONTENTS

LIST OF TABLES

LIST OF ILLUSTRATIONS

LIST OF ILLUSTRATIONS (cont'd)

ACKNOWLEDGEMENTS

This paper reflects the efforts and cooperation of a number of people who helped formulate, conduct, and analyze the many tests presented herein. To this end, I wish to thank the personnel at the MOJAVE STADAN site, without whose aid these tests could not have been performed. I am particularly grateful to Messrs. D. Rau, W. Asplund and G. Shriver of the Westinghouse Electric Corporation for the long hours which they spent conducting tests and analyzing resultant data. I am also most grateful to Mr. J. Baker, Assistant Project Manager, NETCOS Program and to Mr. E. Metzger, the Ground Systems Manager of ATS, for providing me with the opportunity to perform these tests and analysis.

I. INTRODUCTION

The purpose of this report is to summarize the results of initial L-band experimentation utilizing NASA's Applications Technology Satellite ATS-5 and the STADAN ground station located near Barstow, California. Experimentation was performed over a three month period from November 1969 through the middle of February 1970. The objective of the test program was to determine the spacecraft performance characteristics and to perform limited propagation tests. Included in the report are appendices containing information concerning propagation effects as well as measurement techniques.

It is intended that these results will provide some definite characteristics of RF propagation through the atmosphere at L-band frequencies (1650 MHz uplink and 1550 MHz downlink) which can be useful in the development of future spacecraft experiments, primarily experiments involved with air-sea navigation and traffic control.

Originally ATS-5 was designed to operate in an equitorial orbit at synchronous altitude. It was to be gravity gradient stabilized and utilize a high gain phased array antenna for L-band communications. Difficulties were encountered during the orbit injection making it impossible to despin the spacecraft (a maneuver which is a prerequisite to deploying the gravity booms). Therefore, for all practical purposes ATS-5 is spin stabilized. The period of rotation is approximately 787.6 msec (76.2 rpm) with the axis of spin nearly parallel with the earth's spin axis. The spacecraft antenna thus illuminates the earth for a brief time during each spacecraft revolution (the -3 db points illuminate the earth station approximately 52.5 msec each revolution).

This necessitated a change to the original test program which required all spacecraft loop tests to utilize a sampling technique which synchronizes meter readings with the spacecraft spin rate. Therefore the sample time interval becomes a function of the spacecraft antenna pattern and the spin rate, i.e, if less than 3 db variation in signal level is desired, then the sample time will be about 52 msec for an antenna with a 3db beamwidth of 24°.

2. SUMMARY

2.1 Orbital Considerations

The ATS-5 spacecraft was intended to be gravity gradient stabilized in a synchronous orbit. As such, it was equipped with a high gain L-band transmit/receive antenna whose half power beamwidth was sufficient to illuminate the earth.

A synchronous orbit was achieved, although technical difficulties during the spacecraft separation phase of the launch have yielded a spin stabilized spacecraft with a spin period of about 790 ms about an axis of spin approximately parallel with the earth's axis. The spacecraft antenna pattern thus sweeps across the earth each spin period, illuminating each point within its area of coverage for about 52 ms (to the half-power points). The spacecraft orbit is inclined approximately 2.5° with respect to the earth's equatorial plane. This causes a relative north-south motion of the spacecraft as viewed from the earth and results in an apparent displacement of the spacecraft antenna pattern of up to 5°. It should be noted that this displacement of a point on the earth in the spacecraft antenna pattern is orthogonal to the change in antenna pattern due to the spacecraft spin. The effect of the spacecraft orbit inclination is to cause the spacecraft antenna off beam center loss to vary through a 2 db range each 24 hour period.

2.2 Spacecraft Operating Modes

The tests are conducted with the spacecraft in one of three basic operational modes:

1) Narrowband L-L (FM/FM)

   Spacecraft receives at L-band and retransmits at L-band (frequency translation).

2) L-L (SSB/FM)

Spacecraft receives at L-band (SSB) translates to video (500 to 600 kHz) and uses the video signal to modulate (FM) the Spacecraft L-band VCO; the output of which is then translated to L-band for transmission to the earth station.

3) L-C Cross-Strap (SSB/FM)

Spacecraft receives at L-band (SSB), translates to video (500 to 600 kHz) and uses the video signal to modulate (FM) the spacecraft C-band VCO, the output of which is then translated to C-band and retransmitted. When using the C-band downlink, an option exists of either using the C-band high gain or the omni-directional antenna. The use of the latter negates the effect of the spacecraft spin on the downlink.

An additional mode, C-L cross-strap (FM/FM) is also available, however, it is not used in the tests described herein.

2.3 Test Descriptions and Results

Spacecraft Antenna Patterns

The transmit and receive patterns of the spacecraft antenna were measured for several aspect angles of the spacecraft.(the aspect angle changes through 5° in a 24 hour period due to the inclination of the spacecraft orbit). The half-power beamwidth is 24° for transmit and 28° for receive (best estimate).

L-Band Propagation

Four 24 hour tests were performed during which hourly measurements were made of the downlink signal strength. The measurements have been compared with the predicted variation in downlink signal strength due to the orbit geometry. The results correlate to within ±0.3 db which is on the order of the measurement accuracy, thus, no significant diurnal effect is present.

During two of the 24 hour runs, short term fading was measured. Each measurement period (approximately one period each hour) consisted of recording the RMS received signal strength during a 15 msec sample time for each spin revolution of the spacecraft. Each measurement period lasted about four minutes, thus approximately 360 consecutive measurements of received signal were made. The results showed a variation in the received signal level over a four minute period to be less than ±0.3 db, thus no significant signal fading was observed. The results of the propagation tests were compared with link calculations and served to verify the calculated values within the error budget.

Appendix B contains the results of range and range rate tests performed with the ATSR equipment on site. The tests show that the range rate noise errors are less than 1 meter/sec and 0.2 meters/sec for data sampling rates of two and six samples/sec, respectively. Range noise errors were less than 0.7 meters.

Spacecraft Oscillator Frequency Offset

The offset of the spacecraft VCO and master oscillator was measured as a function of time after turn on. The VCO offset from nominal decreased from about -245 kHz at turn on to about -180 kHz 200 minutes later. The master oscillator caused an offset in the earth station baseband signal of about 4 kHz at turn on, and stabilized to about 500 Hz fifteen hours later.

Spacecraft Intermodulation Distortion (SSB/FM)

Two tones, at equal power levels, were transmitted to the spacecraft. The frequency spacing between the tones was varied, as well as the aggregate transmitter power output, and the resulting intermodulation products out of the spacecraft FM modulator were measured. The results indicated that at normal power output levels, the intermodulation products are approximately 26 db below either of the reference tones. This is approximately the same as measured for the transmitter alone, thus indicating that the earth station transmitter is the chief contributor of IM distortion.

Spacecraft Transponder Compression (FM/FM)

The spacecraft transponder compression was measured in the narrow band FM/FM mode and compared to the equivalent prelaunch data. Correlation of the two sets of data provided a means of determining the spacecraft received signal level and thus varifying the uplink predicted values.

Spacecraft SSB/FM Modulator Linearity

The spacecraft FM modulator linearity was measured by transmitting a tone from the earth station at several RF levels and measuring the corresponding received level in an FDM multiplex channel. The received level was converted to the modulation index of spacecraft modulator, which was found to be linear up to a modulation index of 12 radians rms.

Spacecraft Frequency Response

The spacecraft frequency response was measured in both the FM/FM mode and in the SSB/FM modes. In the case of the FM/FM mode, the frequency response is referred to the earth station transmit IF (70 MHz nominal for 1650.0 MHz output). Measured in this manner, the spacecraft center frequency is at 71.25 MHz with a 3 db BW of 2.0 MHz. This corresponds to an L-Band center frequency of 1651.25 MHz. In a similar manner, the frequency response in the SSB/FM mode is measured to be centered at 70.550 MHz with a noise bandwidth of 150 kHz. The half-power bandwidth was about 115 kHz.

Doppler Due to Spacecraft Spin

As the spacecraft antenna sweeps across the earth each spin revolution, the distance between the earth station antenna and the phase center of the spacecraft antenna undergoes a periodic change. This change in range gives rise to a doppler shift of the up and downlink RF carrier frequencies. The maximum amount of doppler shift is a function of the "look" angle of the spacecraft, and is best presented in terms of the antenna pattern. Thus, beginning with an observation point 20 db down on the antenna pattern, the doppler shift varies from an initial value of -1 Hz to a maximum shift of -46 Hz (the doppler shift is non-symmetrical because of the physical configuration of the spacecraft antenna and the corresponding "look" angle).

Multiplex Channel S/N (SSB/FM)

The multiplex channel signal to thermal noise ratio (S/N) was measured to be 36 db (3.1 kHz bandwidth) with an earth station transmitter power output of 50 dbm. The S/N decreased linearly with a decrease in the SSB transmitter power.

Spin Modulation Compensation Test

Due to the spacecraft spin, an earth station signal transmitted at a constant power level will arrive at the input to the spacecraft electronics with amplitude modulation due to the spacecraft antenna pattern. This amplitude modulation may be overcome by modulating the earth station SSB transmitter with the inverse function of the spacecraft antenna pattern in synchronism with the spin rate. This was done utilizing the on-site computer and synchronized timing system with the result that the usable uplink "window" was increased from 52 ms to 100 ms (equivalent half power points).

2.4 Earth Station Equipment Specifications

The earth station equipment specifications are summarized below:

	Transmitter	Receiver
IF frequency (MHz)	70.0	70.0
IF BW (MHz)	7.0	0.5
		2.0
		12.0
		30.0
AGC Time Constant (msec)	---	3
RF frequency (MHz)	1650.0	1550.0
Power output		
Saturated (FM) (dbm)	60	---
Linear (SSB) (dbm)	53	---
Net Antenna gain (db)	33.6	34.7
System Noise Temperature (°K)	---	334

3. SYSTEM DESCRIPTION

3.1 Earth Station Transmit Receive System

The L-band transmit receive system basically consists of a frequency up converter, an intermediate power amplifier, a klystron power amplifier, a 15 foot antenna, a parametric amplifier and a frequency down converter, as shown in figure 1. This system is contained within a mobile van and a portable shelter and located adjacent to the Mojave operations building. This system is interfaced with the existing ATS modulator and demodulator at 70 MHz enabling the station to perform communication experiments with ATS-5 in the L-band frequency range.

The 1650-MHz uplink signal is obtained by a double conversion process. Initially, a 5-MHz frequency standard employing a multiplication process produces two local oscillator frequencies, 380 MHz and 1200 MHz. These signals are mixed with the 70-MHz to produce the 1650-MHz output. This signal is then applied to the intermediate power amplifier which consists of three cavity amplifiers which provide a signal gain of 33 db. The amplified signal is then applied to a power amplifier which is an Eimac/Varian VKL 7764 klystron. This klystron is modified to operate on a center frequency of 1650 MHz with a 7-MHz, 3 db bandwidth. This modified klystron has a saturated power output of 1.0 kw, and is linear up to 200 watts. The amplifier signal is transmitted to ATS-5 via the 15 foot antenna.

The 1550 MHz received signal from ATS-5 is applied to the parametric amplifier. This amplifier consists mainly of a circulator and varactor diode and provides a large gain bandwidth product which is consistent with a low-noise figure. The non-linear capacitance characteristic of the varactor diode is used to transfer power from a high frequency power source (pump oscillator), to the amplified output frequency. The parametric amplifier has a noise temperature of approximately 170°K and a nominal signal gain of 26 db.

This 1550-MHz signal is then applied to a down-converter unit which converts the signal to a 70-MHz IF, which is then interfaced with the station demodulator.

3.2 L-Band Transponder

The L-band transponder is an adaption of the C-band transponder which is a part of previous Application Technology Satellites. The major redesign is in RF portions of the receiver and the transmitter which have new modules operating in the required L-band frequency region. In addition to the RF circuit modifications, several new modules have been added to provide the cross strap and narrow-band FT modes which have not been previously used in the C-band transponders.

A 1650-MHz signal is transmitted from the ground and is received at the satellite by the antenna/transponder according to the mode selected. (See figure 2) The signal is then processed, translated in frequency (1550 MHz) and retransmitted to the ground stations via TWT power amplifiers operating at saturation. The output TWT's may be operated either separately or in parallel thus providing improved reliability through redundancy (separate operation) or an increase of the Effective Radiated Power (ERP) when operated in parallel.

The L-band transponder can operate in four main modes: the wideband frequency translation mode, the narrowband frequency translation mode, the L to L-band multiple access mode and wideband data mode. In addition, the transponder can be cross strapped to provide L to C multiple access and C to L frequency translation modes.

3.3 Modes of Operation

The L-band system utilizes the two major modes of operation Multiple Access (MA) and Frequency Translation (FT) which have been used throughout the five mission ATS program.

The MA experiments will be conducted in two modes: the L-to-L band and the L to C-band cross strap modes.

The FT mode employs two operating bandwidths. The wideband mode has a maximum bandwidth of 25 MHz and is essentially similar to C-band operation. The narrowband mode is identical to the wideband except an improved signal-to-noise ratio is achieved for a single carrier narrowband FM signal by interposing a narrowband filter prior to the limiter amplifier and saturated transmitter. The bandwidth is approximately 2 MHz. In addition, there exists a C to L-band cross strap mode (wideband FT) with an operating bandwidth of approximately 6 MHz.

Figures 3 and 4 illustrate the L-band modes of operation. These figures along with figure 2 which is a detailed block diagram of the L-band Transponder, will be utilized in conjunction with the following mode descriptions.

L to L FT Wideband Mode

This mode functionally, and in its performance characteristics, is identical to the FT mode in the C-band repeater. A single wideband frequency modulated carrier is received at the antenna, filtered in the duplexer (consisting of a circulator and a band pass filter), and amplified in the low noise tunnel diode preamplifier (TDA), see figure 3. The TDA is followed by a bandpass filter which serves the purpose of suppressing TDA noise at the receiver image frequency. The received signal can have a maximum bandwidth of 25 MHz.

After RF preamplification, the signal is converted to IF and further amplified in the pre. inter. and post IF amplifiers. A switchable wideband amplification stage is interposed between the interamp and postamp, in order to be able to switch the narrow band mode out when the WB FT L-L and C-L modes of operation are selected. The signal is amplitude-limited in the limiter amplifier and up-converted to L-band in the high level mixer. An RF power level of 6 to 10 milliwatts at the high level mixer is achieved. This power level however, is not high enough to adequately drive the traveling wave tube transmitter. The required additional gain is provided by a transistor driver amplifier which uses space qualified, high frequency transistors. These amplifiers have adequate gain capability and output power capability well in excess of 100 milliwatts. Since these devices have not been flown in previous ATS spacecraft, the driver amplifier configuration has been given full redundancy. The 25 MHz wide FM signal is retransmitted by the L-band transmitter with no change in modulation.

L to L Narrowband Mode

This mode in all respects is identical to the L to L FT wideband mode shown in figure 3 . The only difference is that it is designed for giving an improved signal-to-noise ratio for a single carrier, narrowband FM signal. This is accomplished by interposing a narrowband amplifier between the interamp and post-amp. This limits the noise bandwidth before the signal and noise are processed through the limiter amplifier and the saturated transmitter. Consequently, this mode can handle lower received signal strengths for the same signal and noise power sharing in the limiter.

In this mode DC switchs route the IF signal (66.1 MHz) through the narrowband IF amplifier. The narrowband filter amplifier module contains a bandpass filter which serves the purpose of restricting channel noise bandwidth. Additional amplification is then obtained in the narrowband post amplifier. The amplified signal is then applied to the post amplifier. The remaining circuitry is identical to that used in the wideband mode.

L to C Cross-Strap Mode

In this mode the L-band receiver will process a number of single sideband or FM signals which are amplified linearly, converted to a video frequency range, and modulated on the C-band repeater VCO. The maximum number of received carriers at L-band is nominally 10, and they cover a total bandwidth which will not exceed 100 kHz. The logic is arranged such that the C-band repeater is in the wideband data mode. The received L-band signals are processed through the RF front end, translated to IF, and amplified (see figure 4). They are passed through the IF narrowband and post amplifiers and are heterodyned to the 500 to 600 kHz frequency range, using four times the master oscillator frequency as a mixing reference frequency. The bandpass filter is a composite of a low pass elliptic function filter and a conventional bandpass filter. The elliptic filter provides a steep skirt at the upper frequency range and the cascaded bandpass filter provides a reasonable roll off at the lower skirt. The elliptic function filter roll off is fast enough to give adequate rejection of image frequency noise (1 MHz above the signal channel) and will thus prevent a degradation in signal-to-noise ratio because of noise fold over. In addition to this L to C mode, a design feature provides a frequency translation mode for a cross strap signal from the C band receiver to the L band transmitter. However this C to L mode is not utilized in this test effort.

L to L Multiple Access Mode

This mode is identical to the L to C Band Multiple Access Cross-Strap Mode except that the C-band repeater circuitry is replaced by the L-band repeater VCO and the L-band transmitter.

Wideband Data Mode

The wideband data mode has the same characteristics in the L-band repeater as in the C-band repeater. It uses the same VCO design, which has identical bandwidth, modulation sensitivity, linearity, etc. as the VCO's in previous ATS repeaters. It is followed by a 25 MHz wide IF amplifier, up-converter and L-band transmitter. The various inputs to the VCO channel selector are cross-strapped between the L-band and C-band repeaters as required, however, each repeater has its own VCO as in previous ATS spacecraft which contained two C-band repeaters.

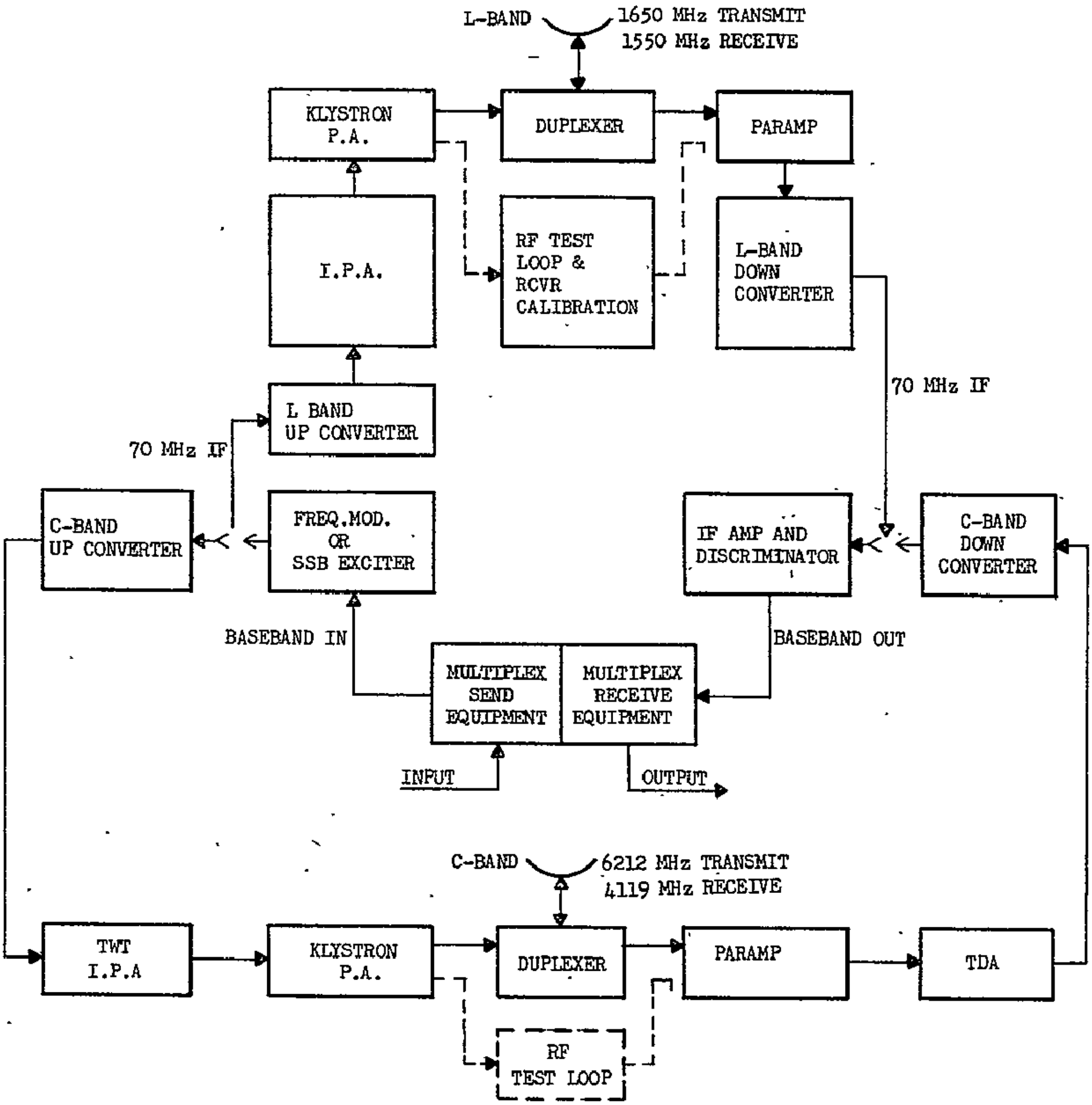

Figure 1. L-Band System Earth Station Block Diagram

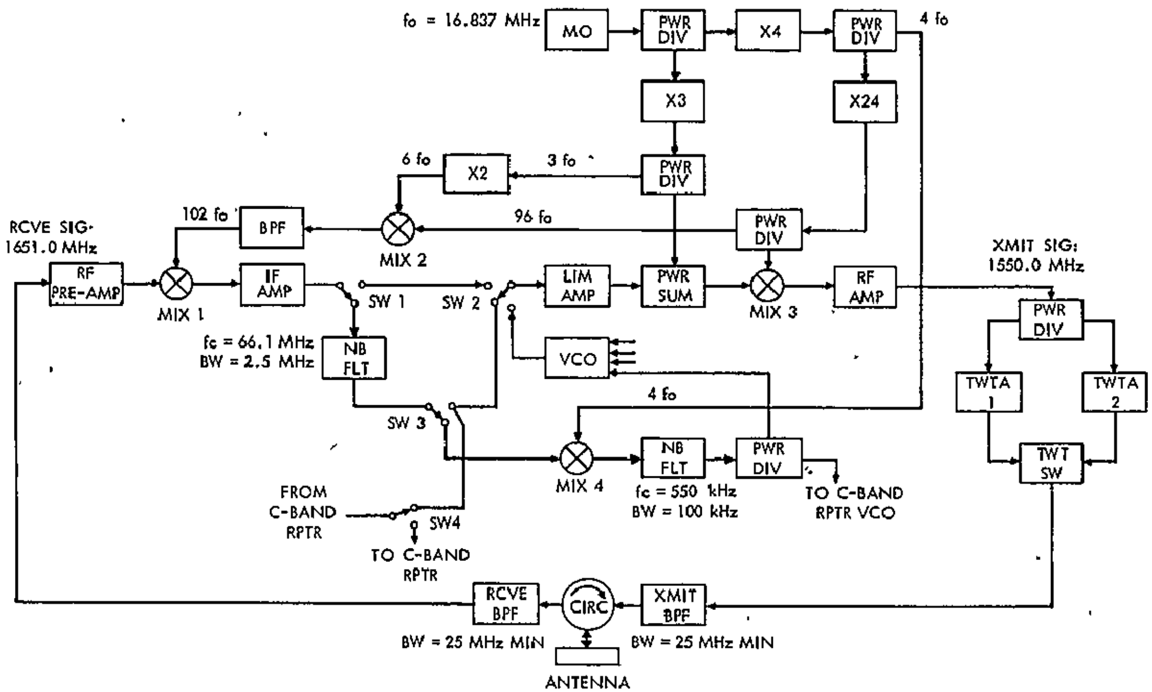

Figure 2. L-Band Transponder Block Diagram

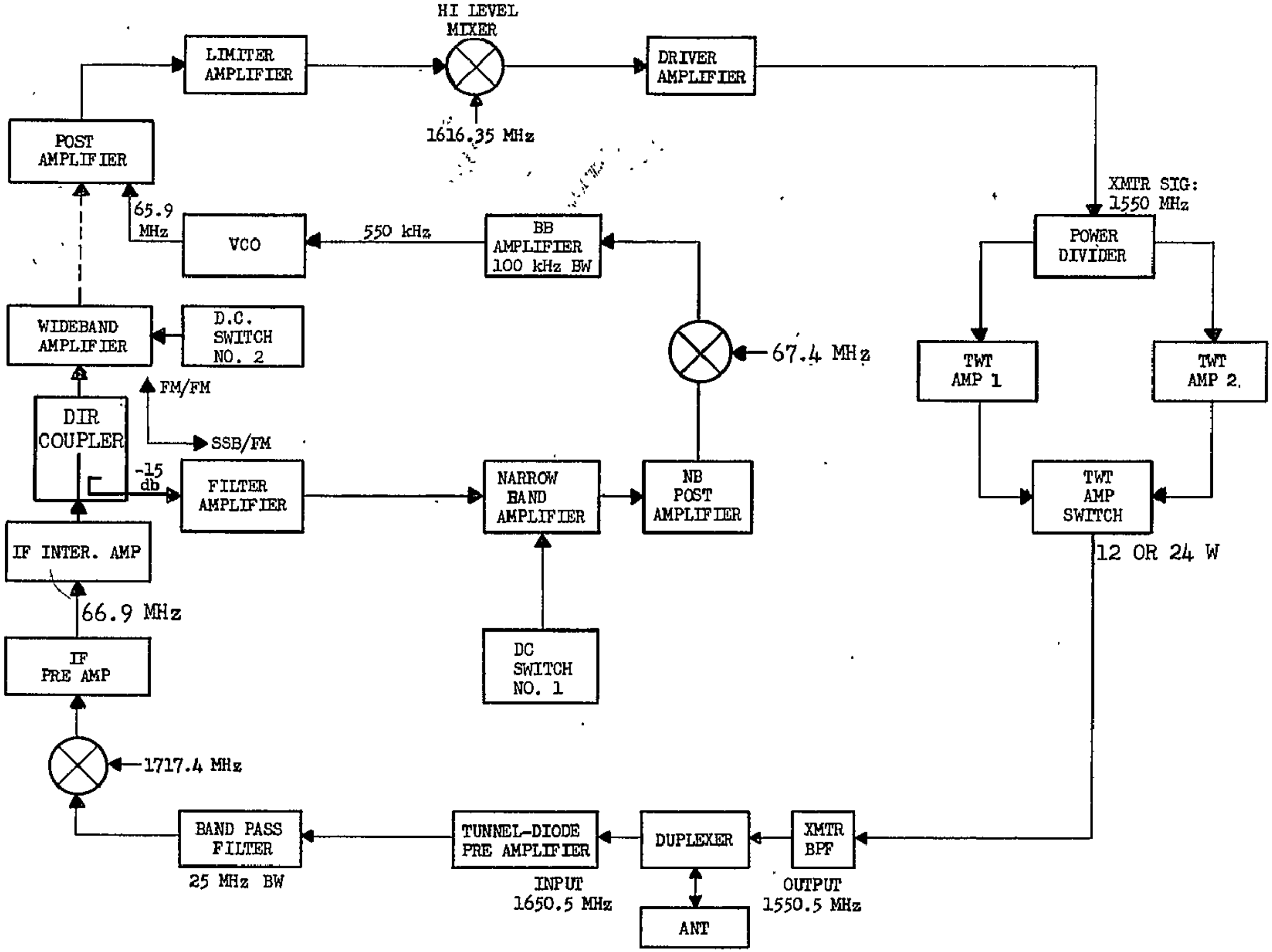

Figure 3. L-to-L-Band Multiple Access Mode

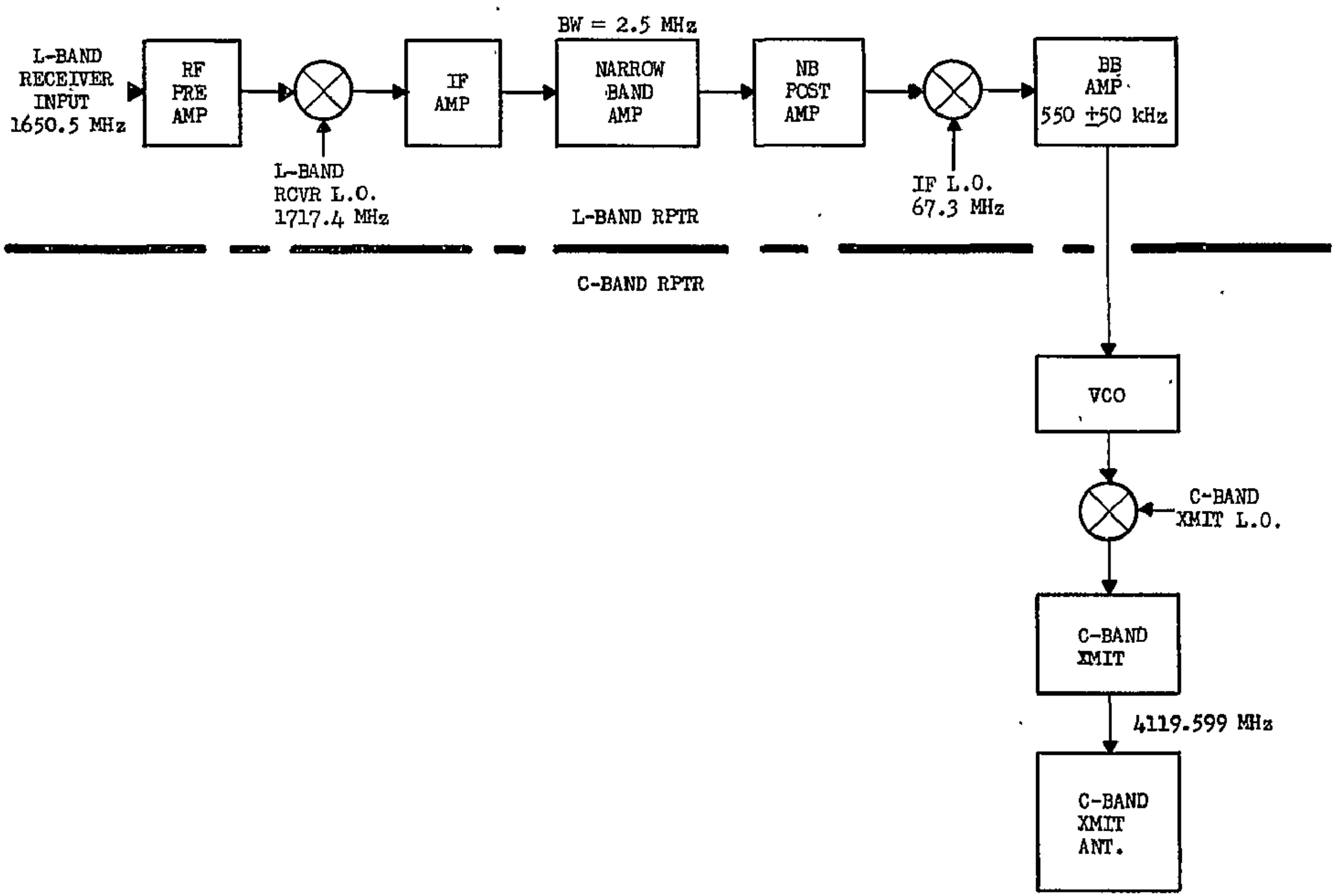

Figure 4. L to C-Band Multiple Access Cross-Strap Mode

4. SPACECRAFT ANTENNA AND PROPAGATION TESTS

4.1 Spacecraft Antenna Patterns

Since technical difficulties have yielded a spinning spacecraft, equipped with antennas that cannot be despun, antenna pattern measurements were necessary in order to determine the duration of various illumination intensities encountered per spacecraft revolution. A brief description of the spacecraft orbit geometry is presented in Appendix 1 in order to show how the signal level varies with time at different places on the earth.

The L-band transmit antenna pattern was measured with the spacecraft in the wideband data mode (WBDM). In the WBDM, a CW signal is generated internally in the spacecraft VCO and then converted to RF for transmission. The spacecraft VCO was unmodulated and the spacecraft transmitter was internally saturated to provide maximum drive to the TWT amplifier (two TWT's were used). The received L-band signal was down converted, passed through an IF filter, and recorded on a strip chart recorder while the spacecraft was spinning at 76.2 rpm.

Figure 5 shows the transmit antenna pattern while table 1 summarizes the antenna parameters. This table is based upon an antenna pattern recorded during a 16 hour series of antenna pattern measurements. The particular pattern analyzed was recorded when the spacecraft was at the most northern point in its orbit, therefore representing the pattern which most nearly passes through the spacecraft antenna boresight. Presented are the earth station received signal levels which correspond to particular points on the pattern. It is instructive to read horizontally across the table at, for instance, the 1 db point. At this level, the antenna pattern is 10° wide, illuminating the earth station for 21.9 msec (based upon a spin rate of 76.2 rpm). The first sidelobes peak at a point about 15.3 db down from the main lobe peak and occur at ± 55 ms from the main lobe peak.

The L-band receive antenna pattern was measured while the system was configured for L-C (SSB/FM) cross-strap operation using the C-band omni-directional or planar array antenna on the downlink. The uplink SSB signal was generated using a 70.533 MHz IF signal. This resulted in a 536 kHz modulation on the C-band downlink which was AM detected and recorded on a strip chart recorder.

The first efforts to record the receive antenna pattern with the C-band omni antenna appeared to be unsuccessful. This was because the recorded pattern showed a "dip" in the main lobe which moved very slowly across the pattern. Subsequent investigation showed that the "dip" was caused by leakage of RF energy into the planar array antenna. With both the planar array and the omni antenna radiating at the same time, phase cancellation and enhancement was causing distortion. At times the cancellation was so severe that the FM receiver operated below threshold. Since the phase relationship between the signals radiated from the two antennas changes with the aspect angle (which changes with time), it was possible to make measurements at a time when distortion was minimum. However, reagardless of the time of measurement, some distortion always appears to be present. In spite of this the general shape of the pattern can be observed and the relative amplitude and position of the side lobes with respect to the main lobe is displayed. The measured receive antenna pattern using the C-band omni antenna is shown in figure 6. Table 2 presents parameters of the antenna pattern and the corresponding illumination time for various points, relative to the peak of the main lobe.

The receive antenna pattern was also measured using the C-band planar array antenna. This permitted much more accurate measurements of the receive pattern main lobe as well as measurements at lower antenna gains. Since, however, the planar array antenna is quite directional, the downlink received signal level dropped below threshold when the earth station was not within the main lobe. As a result only the main lobe of the spacecraft receive pattern could be measured. Figure 7 shows the results of this measurement and table 3 presents the measured parameters. The discrepancies between receive antenna patterns measured using the C-band planar array and the C-band omni antennas is most likely due to the phase distortion already mentioned.

Based on both of the above receive antenna pattern measurement methods, a partial best estimate receive antenna pattern was constructed (See Figure 8). The pattern was constructed using the C-band planar array antenna to provide the shape of the main lobe, while the measurements made using the C-band omni antenna provided the position and amplitude of the side lobes with respect to the main lobe. Table 4 gives the parameters the best estimate pattern.

4.2 L-Band Propagation

The primary objective of this test is to determine uplink and downlink RF path loss at the L-band frequencies. Further objectives of the tests are to determine the time variation of path loss, and atmospheric effects on propagation loss (refer to Appendix B for a presentation of range and range rate tests).

RF path loss, or mean signal attenuation between two antennas, can be predicted from the classical free space attenuation equation. This equation does not include ionospheric and tropospheric effects which may result in signal fading, absorption and scintillation. These may be grouped as atmospheric effects and appear as additional losses. On occasion scintillation may result in signal enhancement due to a "focusing" of the radio signal as it traverses the ionized regions. These factors are frequency dependent and are generally more stable at higher (L-band) than at lower frequencies (VHF band). A mathematical model of the up and down links has been developed from measurements of equipment performance and calculations based on orbit geometry. The elements of the model are used to predict system performance, and hence, are referred to as "Predicted" values. A comparison of measured and predicted values shows how well the measured data supports the chosen model.

These tests attempt to determine whether the measured system performance supports the chosen path model. Since many of the variables are time variant, the tests must be repeated over a period of time to determine the mean value range.

Propagation and diurnal variation were measured during several 24 hour tests. Short term variations on both the uplink and downlink paths showed variations up to ± 0.3 db. Typical recordings of short term variations are shown in figure 9 (chart speed 1 mm/sec.). Each of the strip charts shown in figure 9 represents a portion of the test run. The uplink propagation test provided 531 consecutive measurements of spacecraft received signal strength (approximately seven minutes of data). One measurement was performed each time that the spacecraft antenna illuminated the earth station, thus the sample rate was identical to the spacecraft spin rate. The standard deviation of the uplink data was 0.14 db. Also shown in figure 9 is a portion of a typical downlink propagation record (the standard deviation of this particular record was also 0.14 db, based upon 316 consecutive data points). The downlink received signal strength was recorded for approximately four minutes every hour over a 24 hour test period (actually 34 test records were obtained since it was often possible to perform two test runs within the same hour). Figure 10 shows a plot of the standard deviation versus time for the 24 hour test run. The standard deviation for each four minute test interval is based on an average sample of 285 consecutive data points (3.7 minutes) and varies from 0.09 to 0.37 db with all but four of the intervals having a standard devaiation less than 0.25 db. The average standard deviation of all test intervals was 0.17 db. The results of the test show the maximum fading to occur at about 4:00 p.m. local time (23:30 Z). The local weather conditions (wind velocity, temperature and barometric pressure) were recorded during the 24 hour test, however no correlation with fading activity could be determined.

Diurnal variations due to orbit geometry were calculated to be ± 1 db. Test results indicated a peak-to-peak variation of 2.6 db. Figure 11 shows predicted and measured downlink signal strength versus time for 30/31 January 1970. No 24 hour tests were performed on uplink signal strength however, individual tests indicate that the uplink variation is essentially identical to that measured for the downlink.

Path loss may be measured in the sense that by measuring transmitted and received signal powers and knowing the parameters of the transmitting and receiving antenna systems, the path attenuation can then be computed. These tests, therefore, involve developing techniques for accurately measuring transmitted and received signal powers for both the earth station and the spacecraft, therefore, it is important to know, at the time each measurement is made, what the orientation of each antenna is. To this end, considerable attention has been given to the effects of orbit geometry, off beam center allowance, polarization loss, and measurement of spacecraft received and transmitted power. A brief discussion of these effects is presented in Appendix A

The results of the propagation test are shown in table 6 (L-band-System Link Performance). The table uses the parameters and error budget shown in the table 5 in order to arrive at link performance figures. A description of each table is given below.

Analysis of the results presented in table 6 is best accomplished by first discussing the link parameters and error budget presented in table 5 since these errors represent an integral part of the test results. It should be pointed out that in this section, the term "error" does not mean "mistake" but rather the errors of observation that are a consequence of the inherent, uncontrolled, environmental variability that is part of every data taking process.

Description of Table 5

Table 5 presents a listing of measured or calculated parameters associated with a determination of the propagation tests. Many of the items have been examined in detail in Appendix A and will not be dealt with in detail here.

Referring to Table 5.

1) Unless otherwise stated, all tolerance are assumed ± 0.2 db.

2) The net tolerance are arrived at by RSS (root sum squared) of the individual tolerances.

3) The antenna network losses include all losses between the transmitter power output (or the receiver electronics input) and the antenna feed. All antenna gains and losses are based on actual measurements (prelaunch data for the spacecraft).

4) The tolerance on free space loss is the result of approximately 135 nmi variation in actual slant range to the spacecraft (the range varies from 20,033 nmi to 20, 168 nmi).

5) Polarization loss is explained in Appendix A. The calculated loss is approximately 0.01 db min. to 0.4 max.

6) Spacecraft antenna pointing loss is explained in Appendix A. Ground station antenna pointing loss is relatively small because the L-band antenna is manually slaved to the C-band antenna which is used to track the ATS-5 spacecraft. Before each series of test measurements the pointing angle of the L-band antenna is manually adjusted to correspond to the C-band antenna pointing angle. Since the L-band antenna beamwidth is much larger than the C-band, the resulting error in L-band antenna pointing is small compared with the C-band tracking antenna pointing accuracy.

7) Atmospheric loss is based on tables of ionospheric effects as well as other atmospheric effects likely to occur in the Mojave desert.

8) The spacecraft transmitter power output is determined from prelaunch data.

9) The largest error source is the determination of the uplink received signal strength (SSB/FM mode). This measurement relies upon the sensitivity of the SSB/PM modulator being known. The accuracy of this parameter is specified at ±2.5 db. Future tests are under way to determine this parameter more accurately.

10) The receiver system noise temperature shown is the sum total of the effects of the effective receiver noise temperature and the antenna noise temperature, <u>PLUS</u> the effect of the receive network loss.

<u>Discussion of Table 6</u>

The propagation tests are primarily concerned with determining the propagation effects, at L-band, between the earth station and the spacecraft. This involves a determination of transmitter power output, receiver input power, and net antenna gains. Once these parameters are established, the net transmission loss may be determined.

Considering the SSB uplink, we see that a predicted SSB transmitter power of 32.3 dbm is required in order to produce the nominal level of -113.0 dbm at the spacecraft when the spacecraft is in its southern-most position. The level of -113.0 dbm is selected because that is the level specified (±2.5 db) by the design specification which is to provide 1.0 rad. rms mod index in the FM downlink. Using this figure, the appropriate transmission losses are calcualted.

Following the same sequence, the measured uplink SSB transmitter power required to produce a mod index of 1.0 rad rms in the downlink (as measured with the spectrum analyzer) is 29.1 dbm. The test was actually performed at a modulation index of 2.4 radians peak (first carrier null) and normalized to 1.0 radians rms). Assuming that the SSB/FM modulator sensitivity is nominal (i.e., -113.0 dbm), it is then possible to calculate the net transmission loss. The measured and predicted transmission losses agree within 3.2 db, which is within the total tolerance of the measurements (±2.7 db on predicted and ±0.8 db on measured total to a net tolerance of ±3.5 db). The measurement indicates that the SSB/FM modulator is near the more sensitive end of its allowable range.

The FM uplink columns show the predicted and measured link performance. The spacecraft transponder compression was measured in the narrow band FM/FM mode and compared to the equivalent prelaunch data. Correlation of the two sets of data provided a means of determining the spacecraft receive signal level. The predicted and measured values agree within 0.5 db.

The FM downlink measured values appear to be in closer agreement with the predicted values than was the case with the uplink. Using the same procedure as before to calculate net transmission loss from measured data, it is found that the result is within 0.5 db of the predicted value (the tolerance between the two values is ±0.8 db and ±1.1 db for the measured and predicted values, respectively, for a net tolerance of ±1.9 db).

The mathematical model of the system link parameters has been verified by propagation measurements, however, the precision to which the model is known is not sufficient to detect small discrepancies between measured and predicted values.

TABLE 1. ATS-5 L-BAND TRANSMIT ANTENNA PATTERN
① (S/C TO EARTH STATION LINK)

		Earth Station Received Signal Strength ② (dbm)	Antenna Pattern Beam Width	Time Earth Station is Illuminated ③
Main Beam	Max	-99.0 dbm	—	
	-1 db	-100.0 dbm	10°	21.9 msec
	-3 db	-102.0 dbm	24°	52.5 msec
	-6 db	-105.0 dbm	36.0°	78.7 msec
	-10 db	-109.9 dbm	48°	105.0 msec
1 st Side Lobes (Max)				
	-15.3 db	-113.5 dbm	—	—
(side lobes occur ±55° from peak of main beam)				

① At maximum Northern excursion of S/C

② Power at input to Earth Station Preamp (Earth Station Antenna Gain = 35.7 db)
S/C Transmitter Power = 24 Watts (Two TWT's)

③ Based on a S/C spin period of 787.6 ms (76.2 rpm)

TABLE 2. ATS-5 L-BAND RECEIVE ANTENNA PATTERN (L TO C CROSSTRAP MODE, C-BAND OMNI ANTENNA)

		Antenna Pattern Beam Width	Time Earth Station is Illuminated*
Main Beam	-1 db	10°	21.9 msec
	-3 db	23°	50.4 msec
	-6 db	35°	76.6 msec
	-10 db	48°	105.0 msec
1st Side Lobes (Max)			
	-13.7 db and -15 db		
	(side lobes occur at +57° and -48° from main beam peak)		

*Based on a S/C spin period of 787.6 mx (76.2 rpm)

TABLE 3. ATS-5 L-BAND RECEIVE ANTENNA PATTERN (L TO C CROSS STRAP MODE, PLANAR ARRAY)

		Antenna Pattern Beam Width	Time Earth Station is Illuminated*
Main Beam	-1 db	15°	32.8 msec
	-3 db	28°	61.3 msec
	-6 db	37°	81.0 msec
	-10 db	45°	98.5 msec

*Based on a S/C spin period of 787.6 ms (78.2 rpm)

TABLE 4. ATS-5 L-BAND RECEIVE ANTENNA PATTERN (BEST ESTIMATE)

		Antenna Pattern Beam Width	Time Earth Station is Illuminated*
Main Beam	-1 db	15°	32.8 msec
	-3 db	28°	61.3 msec
	-6 db	37°	81.0 msec
	-10 db	45°	98.5 msec
1 st Side Lobes (Max)			
	-13.7 db and -15 db		
	(Side lobes occur at ±52° from main lobe peak)		

*Based on a S/C spin period of 787.6 ms (76.2 rpm)

TABLE 5. L-BAND SYSTEM LINK PARAMETERS AND ERROR BUDGET*

		UPLINK (1650 MHz)		DOWNLINK (1550 MHz)
		SSB	FM	FM
TRANSMIT ANTENNA GAIN	(db)	35.7	35.7	14.0
TRANSMIT NETWORK LOSS	(db)	2.1	2.1	2.0
RECEIVE ANTENNA GAIN	(db)	15.0	15.0	35.7
RECEIVE NETWORK LOSS	(db)	2.3	2.3	1.0
NET ANTENNA GAIN	(db)	46.3 ±0.4	46.3 ±0.4	46.7 ±0.4
FREE SPACE LOSS	(db)	188.4	188.4	187.8
POLARIZATION LOSS	(db)	0.2	0.2	0.2
S/C ANT. POINT LOSS**	(db)	0.3 to 2.3±0.5	0.3 to 2.3±0.5	0.3 to 2.3±0.5
EARTH STATION ANT. POINTING LOSS	(db)	0.5 ±0.5	0.5 ±0.5	0.5 ±0.5
ATMOSPHERIC LOSS	(db)	0.2	0.2	0.2
NET PROPAGATION LOSS	(db)	189.6 to 191.6±0.8	189.6 to 191.6±0.8	189.0 to 191.0±0.8
TRANSMITTER POWER OUTPUT*** (measurement accuracy)	(dbm)	±0.5	±0.5	±0.5
RECEIVED SIGNAL STRENGTH			-83.3 to -85.3	-98.9 to -100.9
(measurement accuracy)	(db)	±0.5	±0.5	±0.5
(SSB/FM mod. sensitivity)	(db)	±2.5	—	—
NET ERROR IN DETERMINATION OF LINK PERFORMANCE	(db)	±2.7	±1.1	±1.1
EFFECTIVE RECEIVER NOISE TEMP (°K)		1470	1470	170

* Unless otherwise indicated, all parameters are assumed accurate to within ±0.2 db.

** The S/C antenna point loss is a function of the S/C orbit geometry and is predictable as a function of time.

*** The ground station transmitter power output is adjusted to establish a predetermined S/C received signal, and is therefore dependent upon orbit configuration and system operating mode.

TABLE 5. L-BAND SYSTEM LINK PARAMETERS AND ERROR BUDGET (cont'd)

RECEIVE ANTENNA NOISE TEMP (°K)	290	290	55
RECEIVE SYSTEM NOISE TEMP (db°K)	32.5	32.5	25.3
NOISE POWER DENSITY (dbm/Hz)	-166.1	-166.1	-173.3

TABLE 6. L-BAND SYSTEM LINK PERFORMANCE*

	UPLINK (1650 MHz)				DOWNLINK (1550 MHz)	
	SSB		FM(NB)		FM	
	Measured	Predicted	Measured	Predicted	Measured	Predicted
TRANSMITTED POWER (dbm)**	29.1 ±0.5	32.3	60.0 ±0.5	60.0	43.4 ±0.5	43.4
NET ANTENNA GAIN (db)	46.3 ±0.4	46.3	46.3 ±0.4	46.3	46.7 ±0.4	46.7
RECEIVED SIGNAL (dbm)***						
S/C at max N	-111.0 ±0.5	-111.0	-82.8 ±0.5	-83.3	-98.4 ±0.5	-98.9
S/C at max S	-113.0 ±0.5	-113.0	***	-85.3	-101.0 ±0.5	-100.9
NET TRANSMISSION LOSS (db)						
S/C at max N	186.4 ±0.8	189.6	189.1 ±0.8	189.6	188.5 ±0.8	189.0
S/C at max S	188.4 ±0.8	191.6	***	191.6	191.1 ±0.8	191.0
RECEIVED NOSIE POWER DENSITY (dbm/Hz)	-166.1	-166.1	-166.1	-166.1	-174.2	-173.3
LINK C/N_o (maximum value) (db)						
S/C at max N	55.1 ±0.8	55.1	83.3 ±0.8	82.8	75.8 ±0.8	74.4
S/C at max S	53.1 ±0.8	53.1	***	80.8	73.2 ±0.8	72.4

* Tolerance of predicted values is ±2.7 db on SSB uplink, ±1.1 on the FM uplink, and 1.1 db on downlink (refer to Table 5).

**Uplink transmit SSB power required for mod index of 1.0 rad rms (S/C at max S) assuming nominal sensitivity of SSB/FM modulator.

***S/C received power not determined for FM (NB) mode.

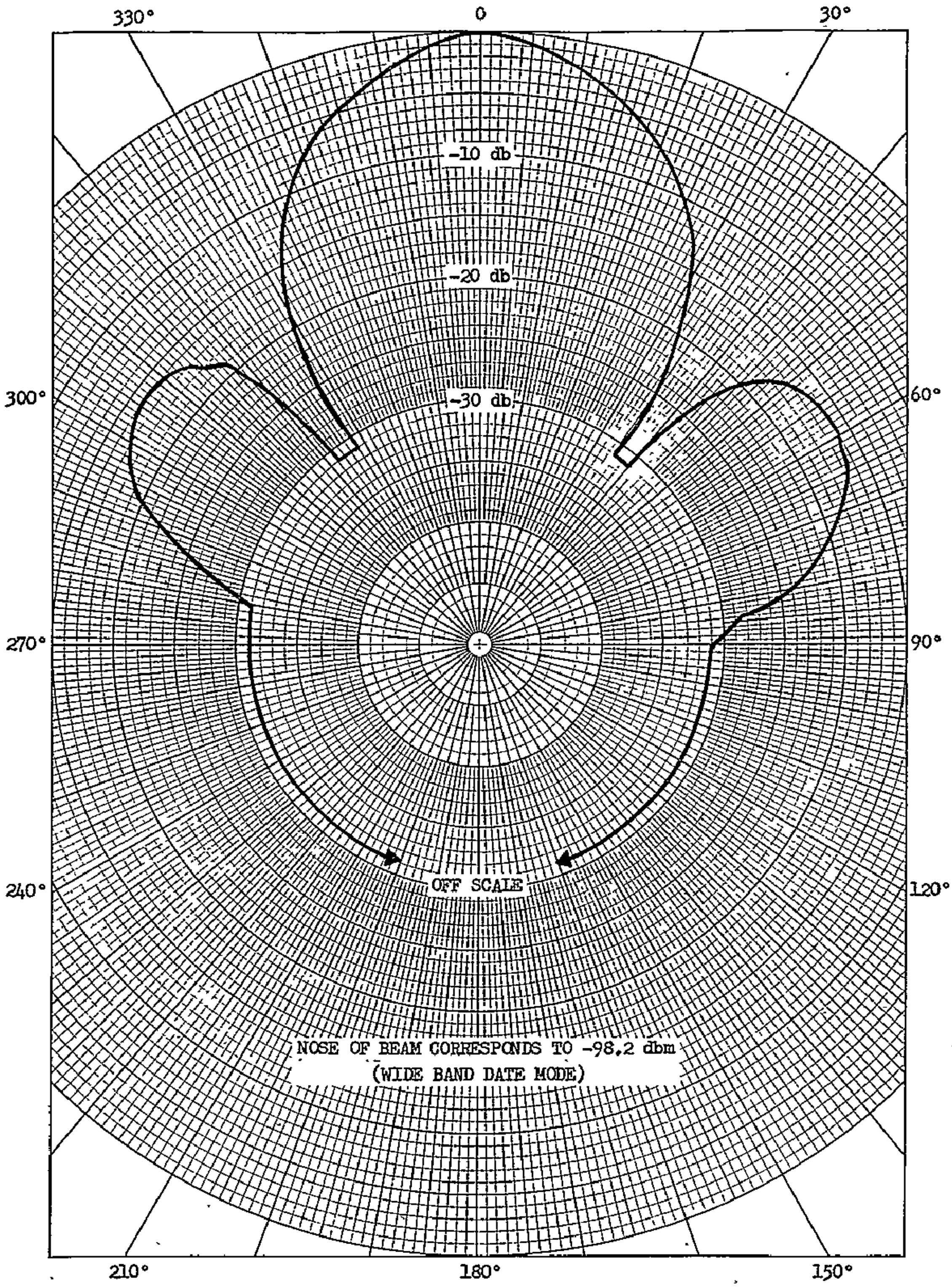

Figure 5. ATS-5 L-Band Transmit Antenna Pattern

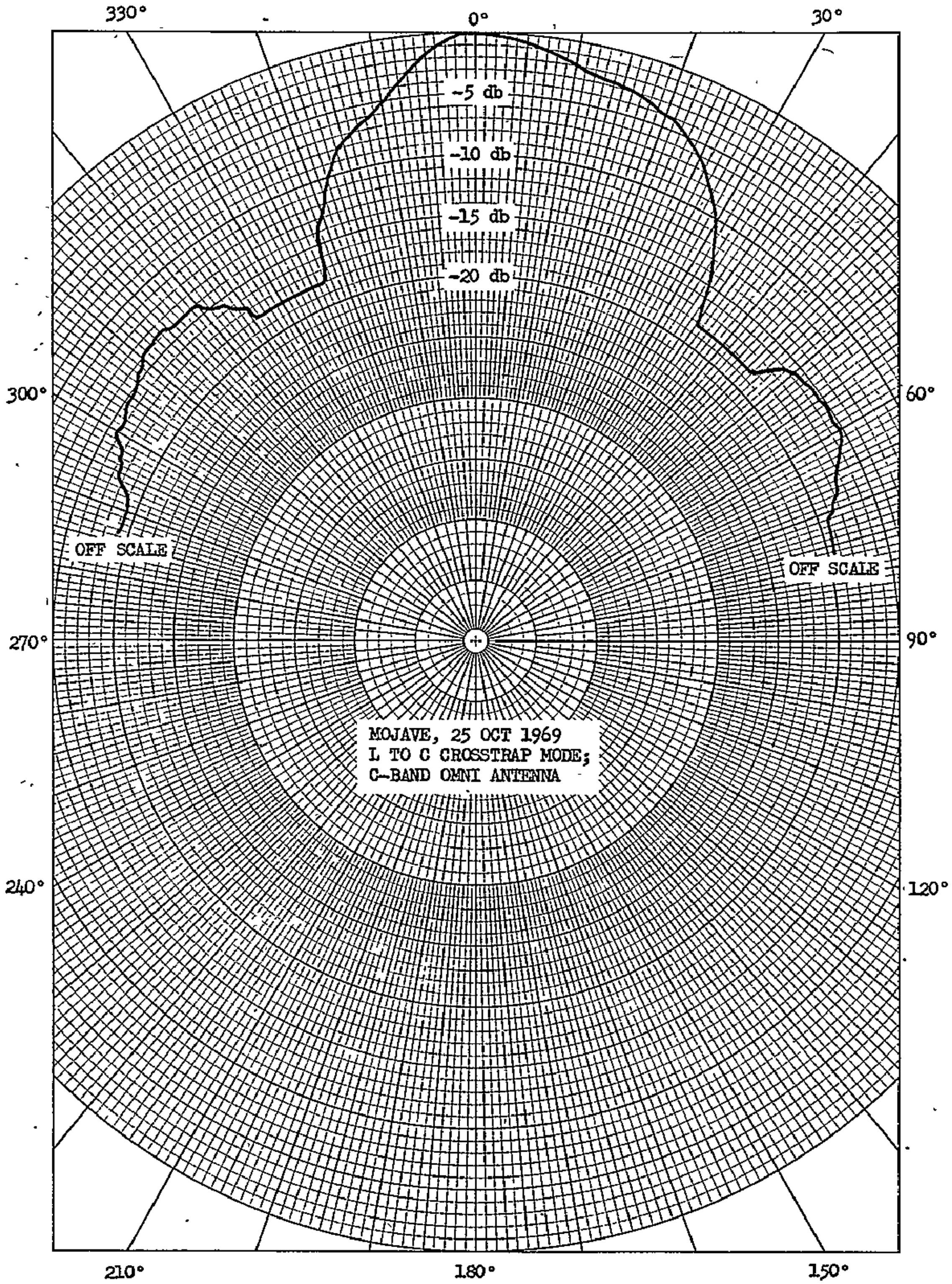

Figure 6. ATS-5 L-Band Receive Antenna Pattern (C-Band Omni Antenna)

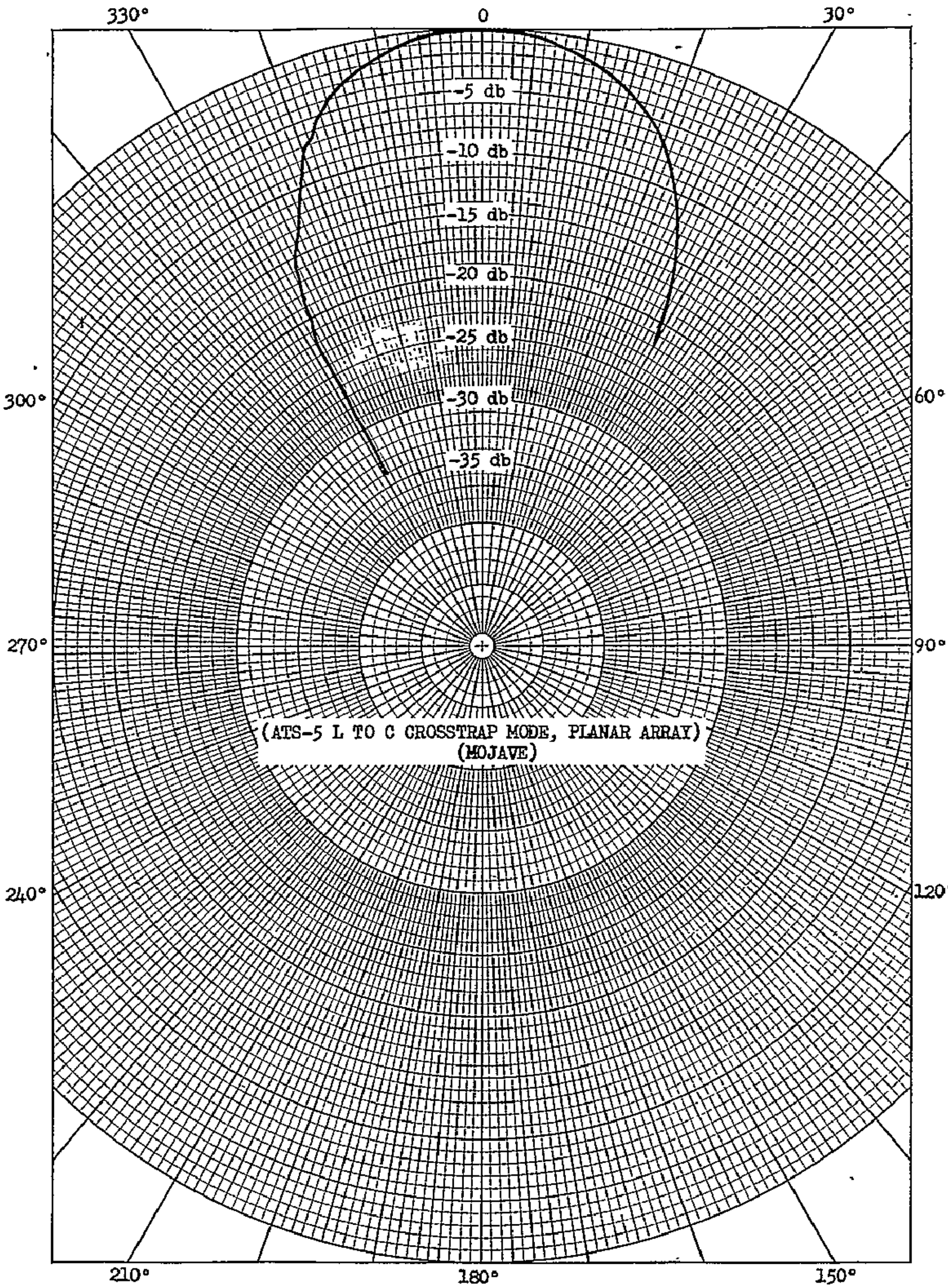

Figure 7. ATS-5 L-Band Receive Antenna Pattern
(C-Band Planar Array Antenna)

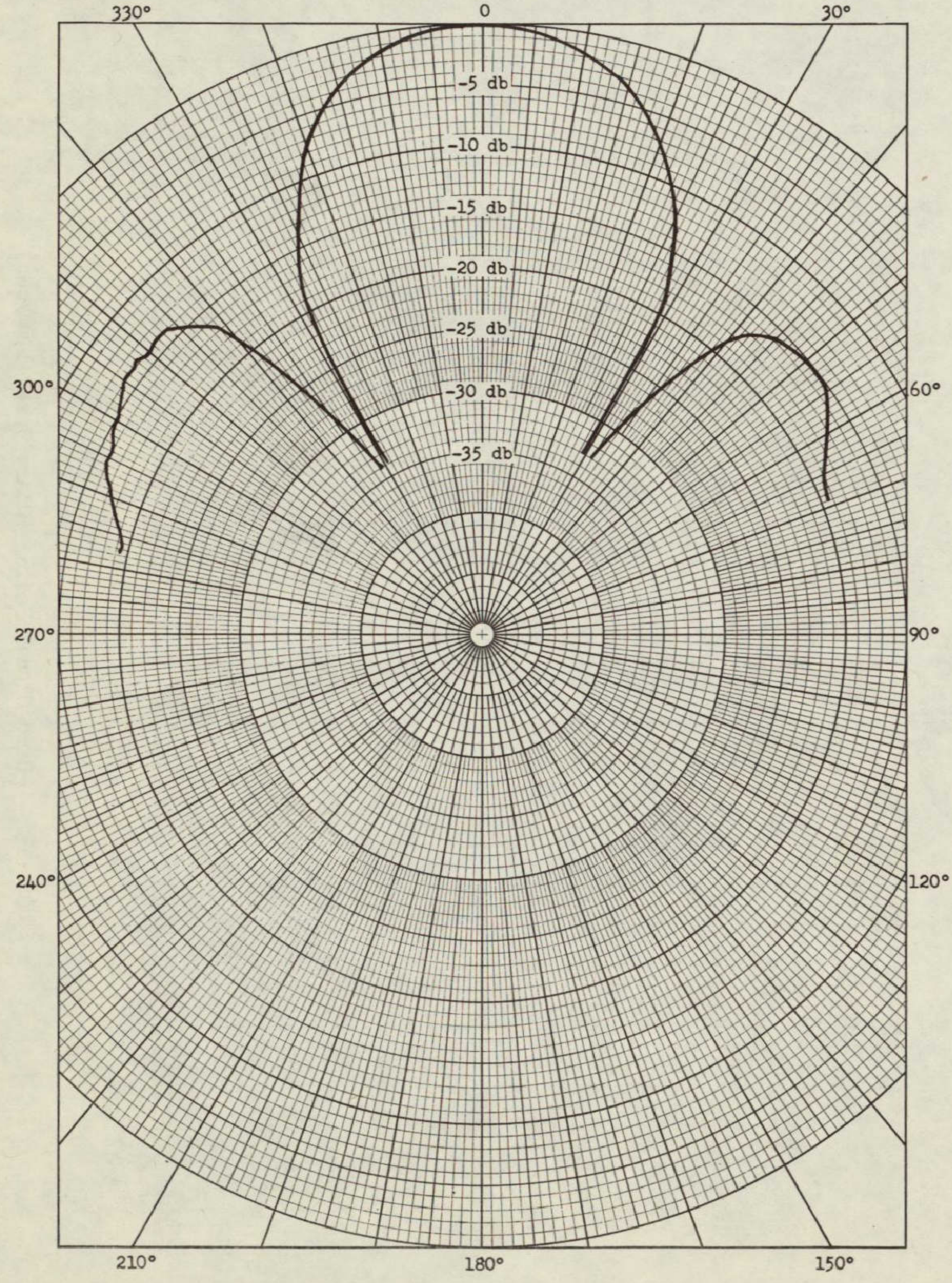

Figure 8. ATS-5 L-Band Receive Antenna Pattern (Best Estimate)

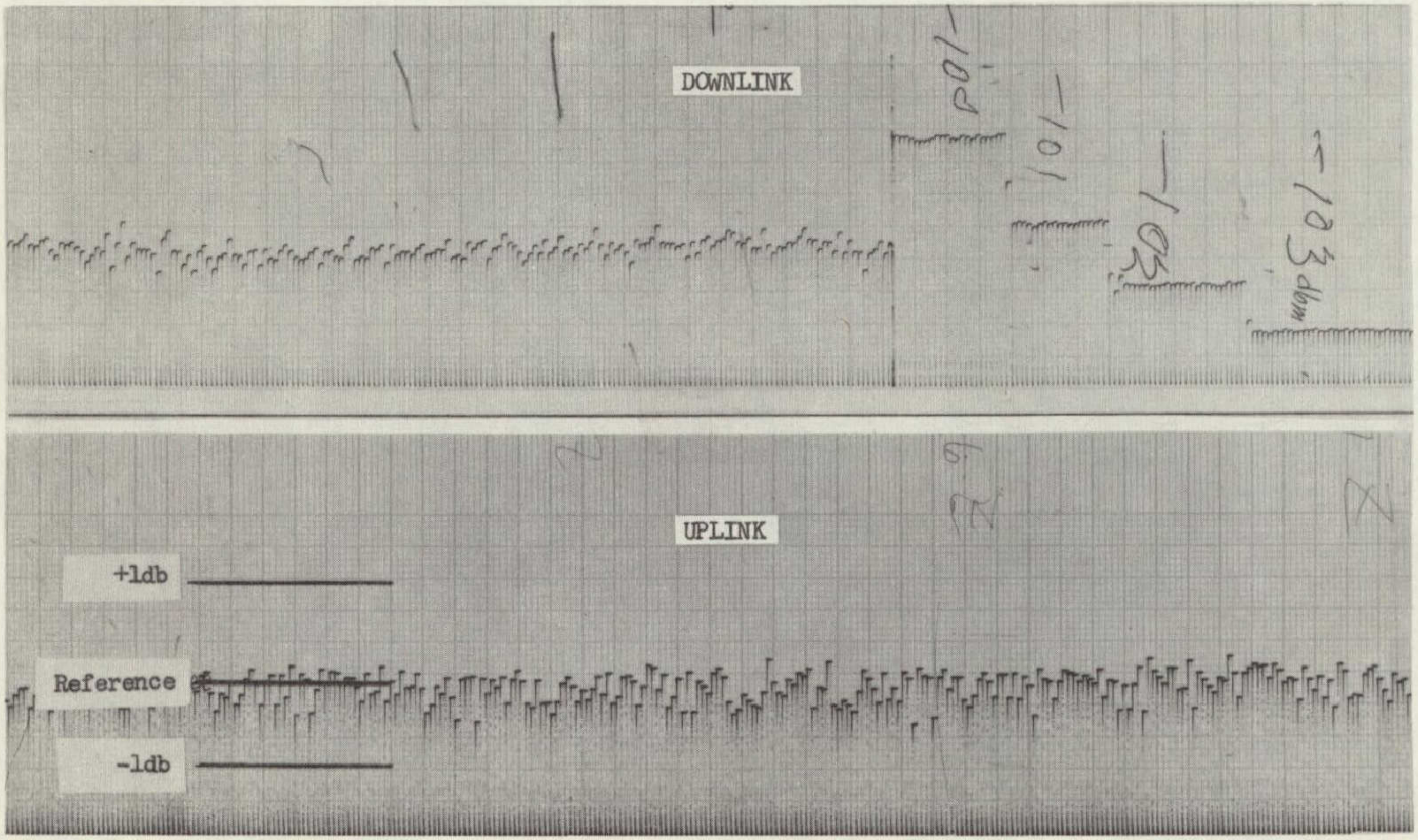

Figure 9. L-Band Signal Fading (Chart Speed 1 mm/sec)

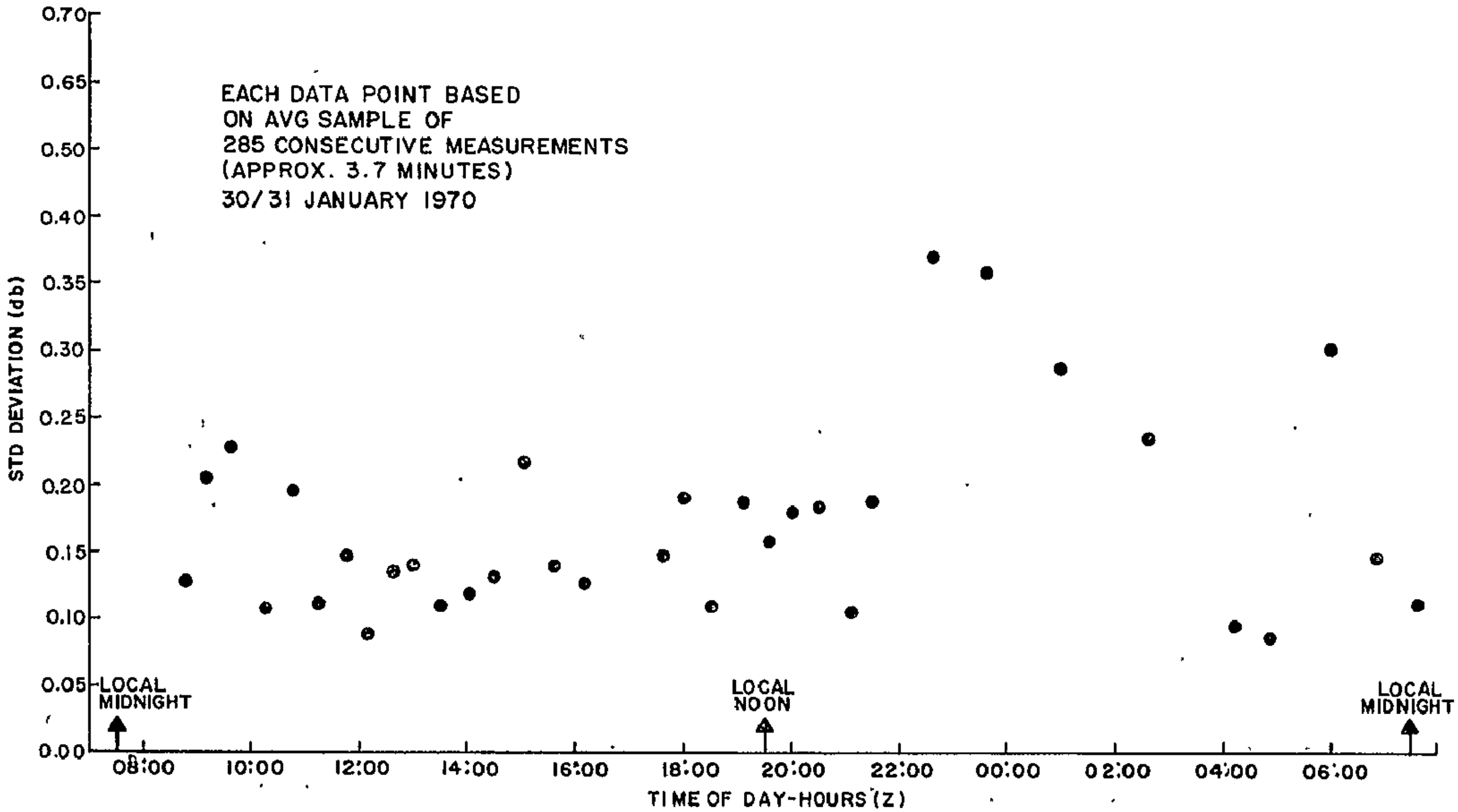

Figure 10. L-Band Downlink Propagation (1550 MHz)

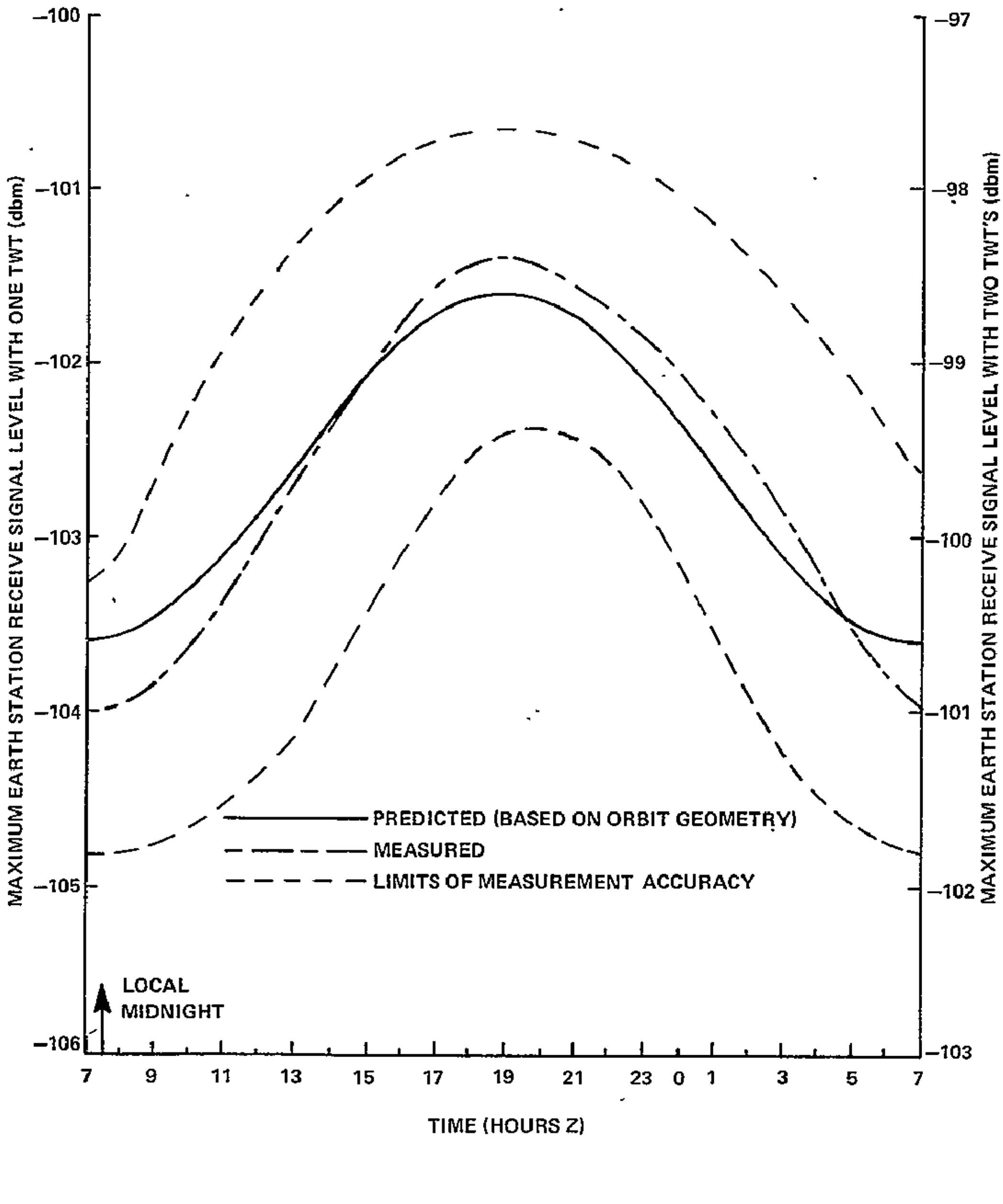

Figure 11 Downlink Received Signal Strength Versus Time

5 SPACECRAFT PERFORMANCE CHARACTERISTICS

5.1 Spacecraft Oscillator Frequency Offset

VCO Offset

The spacecraft VCO frequency offset as a function of time after turn-on is shown in figure 12. The frequency of the spacecraft VCO is determined by monitoring the downlink IF frequency while the spacecraft is in the Wideband Data Mode (WBDM). In this mode a baseband signal is generated internally in the spacecraft. Any frequency drift or offset is due to spacecraft VCO or master oscillator. The spacecraft VCO's nominal operating point is about 65.89 MHz, with any offset being translated to RF. In the earth station receiver the RF offset is translated to the receiver's 70 MHz IF. Master oscillator offset measurements show that the master oscillator frequency offset and drift is negligible when compared to VCO frequency offset and drift.

The time period covered in figure 12 is from 11 minutes after turn-on to slightly over 3 hours after turn-on. At eleven minutes after turn-on the frequency was about 245 kHz below its nominal center frequency. Each successive measurement indicated that the frequency offset was diminishing. However, at 192 minutes after turn-on the frequency offset was still at -184 kHz.

The VCO frequency offset may be exeessive at times for certain applications. The amount of frequency offset that can be tolerated is also dependent upon the bandwidth of the IF filter. If the frequency offset is considered excessive for the desired application two alternatives are available. First the VCO could be turned on long enough prior to transmission time to allow the offset to come within desired tolerances, or, the down-converter local oscillator may be offset in order to position the IF to the desired frequency.

Master Oscillator Offset

The L-band Master Oscillator frequency offset as a function of time after turn-on is shown in figure 13. In the MA (SSB/FM) mode, the incoming SSB signal is hetrodyned to baseband via a double mixing process within the spacecraft. The local oscillator for each mixing operation is derived from the spacecraft master oscillator. In one case the master oscillator frequency is multiplied by 102, and in the other case by 4. The mixing is performed in such a way that the frequency errors caused by the master oscillator are non additive. This causes the frequency error in the baseband signal to be 98 times the error in the master oscillator. The resulting baseband signal is used to frequency modulate the spacecraft VCO, and thus undergoes no further frequency errors. There is, therefore, a 1:98 ratio between the spacecraft master oscillator frequency offset and the earth station receiver baseband frequency offset. For example, if the spacecraft master oscillator frequency is 10 Hz high, the baseband frequency will be 980 Hz high. The frequency offset due to the spacecraft master oscillator is measured by transmitting a tone from the earth station corresponding to a particular baseband frequency. The frequency of the earth station baseband tone, after passing through the spacecraft, is measured to determine the master oscillator frequency offset. This test is of particular significance when transmitting FDM where a few hundred Hz baseband frequency offset may be significant.

The C-band and the L-band spacecraft transponders each have their own master oscillators. If desired, these master oscillators may be kept on even though the associated spacecraft transmitter is off. This would allow the master oscillator to stabilize in advance of a particular test.

As shown in figure 13, a baseband frequency offset of slightly more than 4 kHz occurs at about 1.5 hours after turn-on. This frequency offset decreases with elasped time after turn-on. However, after operating for about 17 hours the baseband frequency is still nearly 400 Hz above the desired frequency.

The master oscillator is much more stable than the L-band VCO. Therefore, the baseband frequency offset caused by the master oscillator may be neglected when operating in the wideband data mode. However, when transmitting FDM, either the earth station transmitter local oscillator will have to be offset, or a long warm-up period will be required for the spacecraft master oscillator to stabilize. In either case, it may be necessary to track (either manually or automatically) the baseband frequency drift. Automatic tracking would probably involve the transmission of a suitable pilot tone.

5.2 Spacecraft Intermodulation Distortion

The objective of this test is to measure the 3rd and 5th order intermodulation products. This test is performed by injecting two signals into the earth station transmitter IF. The signals pass through the remainder of the transmitter system, the spacecraft, and the front end of the earth station receiver. This is the L-band receiver in the L-L band mode and the C-band receiver in the L-C crosstrap mode. The intermodulation products are measured in the receiver IF via a spectrum analyzer or a tuned receiver.

Intermodulation Distortion in the SSB/FM mode may be measured while employing a 12 MHz or a 2 MHz filter in the earth station L-band receiver IF section. If the 12 MHz filter is used the system is thermal noise limited, thus, intermodulation products are not the limiting factor. When the 2 MHz is used high 3rd order intermodulation products appear.

The SSB/FM mode of operation was designed primarily for the transmission of ranging tones where intermodulation products may be of little significance since the ranging tests are conducted using a narrowband phase-lock loop. Intermodulation products could hinder acquisition of the proper signal, however, after lock-up to this signal intermodulation products are outside of the bandwidth in use. Two-Tone Intermodulation tests were performed using the L-C cross-strap mode (SSB/FM) with a 30 MHz BF filter in the receiver IF. In this configuration, the third order two tone intermodulation products were measured to be in the order of 26 db below either tone. This is approximately the same as measured for the transmitter alone, thus indicating that the transmitter is the primary source of IM distortion.

5.3 Spacecraft Transponder Compression

The compression curve for the spacecraft transponder (narrow band, FT mode) is shown in Figure 14. Both prelaunch and post-launch data are presented. The latter was accomplished by varing the uplink power level from 30 dbm to 52 dbm and recording the received downlink power. The saturation point is defined as that spacecraft input power level which when increased by two db, results in a one db increase in spacecraft power output (also referred to as the one db compression point). The one db compression point was found to be -103.5 dbm.

The two compression curves (pre and post launch) may be utilized to verify the link calculations, since, when overlain for a best fit, they correlate earth station transmitter power output and spacecraft power input.

5.4 Spacecraft SSB/FM Modulator Linearity

The linearity characteristic of the spacecraft FM modulator is shown in figure 15. The system is in the SSB/FM mode with the ground receiver utilizing the 30 MHz IF filter. The linearity characteristic will be given in terms of the functional relationship between the S/C received power (Prs) and the resulting modulation index (M). For this test, an L band frequency was employed on both the up and down link paths (1650 MHz and 1550 MHz, respectively).

A 533 kHz modulating signal was transmitted via the SSB uplink for discrete values of ground transmitter power (Ptg). For each power value, a corresponding value for the S/C received power (Prs) was computed utilizing link calculations. For each value of Ptg a corresponding ground received test tone power level was measured. This power level varies directly with M^2. From the above relationships it was then possible to develop the desired function. To determine specific values of M for a given P_{rs}, pre-launch measurements of S/C input power and the resulting value of M were employed. From these measurements it was determined that for an input power level of -113 dbm, an M of 1.0 radian rms results for a modulating frequency of 533 kHz.

The resulting test data is shown in figure 15 as a plot of M versus Prs. Since, ideally, M varies as the square root of Prs (linearly with voltage), a plot of M versus Prs an semi-log paper will be a straight line. The point at which the function deviates from a straight line defines the linear operating region of the FM modulator. As shown in figure 15, the upper limit of the linear region occurs at an M of 12 radians rms for a Prs of about-92 dbm. For this value of M, the corresponding rms frequency deviation is 6.4 MHz.

No masking effect of the FM modulator characteristics due to IF bandwidth limitations on the ground received test tone power level was present in this test. This follows from the fact that the required IF bandwidth for an M of 12 and a fm of 533 kHz is 13.9 MHz. A 30 MHz filter was employed in the ground receiver; hence, the curve in figure 15 truly represents the desired operating hcaracteristics of the S/C FM modulator.

5.5 Spacecraft Frequency Response

The frequency response of the S/C system was measured for operation in the FTNB mode with a 2.5 MHz IF filter. The ground transmitter IF frequency was varied over a range of 69.8 MHz to 73.5 MHz. The corresponding ground received IF tones were inserted into an amplitude detector whose output was then displayed on a calibrated strip chart. The resulting peaks of the recorded signal were employed as a measure of the frequency response. Bandwidth limitations in the ground units were minimized by operating these units with relatively wideband filters and also by taking corresponding readings in a ground loop configuration and subtracting the effects from the overall S/C loop response.

Figure 16 shows the results of the frequency response test. The width of the response at the 3 db and 1 db points are 2 MHz and 1.3 MHz, respectively. It is noticed that the skirt response is unsymmetrical relative to the center frequency. On the low and high side of the response the average shape of the roll-off is 12 db/MHz and 7 db/MHz, respectively. This unsymmetrical shape agrees with the pre-launch response measurements.

The frequency response of the ATS-5 system operating in the SSB/FM mode is shown in figure 17. As shown, the 3 db BW in about 115 kHz (Further analysis of the data showes that the noise power bandwidth is 150 kHz). The test was performed by transmitting a tone from the earth station which, when hetrodyned by the spacecraft mixers, would lie within the IF filter preceeding the spacecraft VCO. The frequency of the transmitted tone was adjusted in 10 kHz steps over the baseband frequency range in the spacecraft. The tone, after passing through the baseband filter was then used to modulate the spacecraft VCO. The VCO frequency was converted to L-band and transmitted to the earth station. The modulation index of the downlink signal was thus directly proportional to the signal strength of the modulating signal. At the earth station, the downlink signal was FM detected, and the power level of the modulating signal was measured.

5.6 Spin Doppler

Because ATS-5 has a spinning antenna which has a phase center offset from the spin axis, spin doppler and doppler rate will be present on all signals passing through the transponder. The doppler is proportional to (1) The RF frequency and (2) the projection of the velocity vector of the antenna phase center onto a line extending from the ground station to the spacecraft antenna phase center. The doppler rate (rate of change of frequency shift) is proportional to (1) the RF frequency and (2) to the projection of the acceleration vector of the antenna phase center onto the line of sight between the ground station and spacecraft antenna phase center.

In figure 18 the spacecraft antenna phase center velocity and acceration vectors are shown in relationship to the relative positions of the ground stations with respect to the spacecraft when the ground station is illuminated by various portions of the spacecraft antenna pattern. For example, in position #5 the ground station is almost directly in line with the velocity vector, therefore the absolute maximum doppler due to spacecraft spin will be present on the RF frequencies being measured at this time. In this case, the velocity vector is directed away from the earth station, thus causing a negative doppler shift.

One way doppler may be calculated using the following formula:

$$f_d = \frac{f_c \, RW \cos \Theta_1}{C}$$

where f_c is the carrier frequency in Hz, R is the radius of the phase center of the antenna from the spin axis of the spacecraft in ft., W is the angular frequency of the spinning spacecraft in radians/sec, C is the velocity of light in ft/sec, and θ_1, is the angle between the velocity vector and the ground station line of sight to the spacecraft. To calculate the two way doppler the uplink and downlink must be calculated separately because of the different frequencies involved, and then the two doppler frequencies are added.

Two way doppler was measured by mixing a recovered 70 MHz tone which was sent through the spacecraft repeater with a locally generated tone of nearly 70 MHz. The recovered tone will have 2-way doppler present, so that the resultant tone after mixing will be doppler plus some frequency offset. The resultant tone was monitored on an oscilloscope; patterns of some of these measurements are shown in figure 19.

Doppler rate can be calculated using the following formula:

$$\dot{f}d = \frac{fc\ (R\ W^2 \cos\ \theta_2)}{C}$$

where f_c, R, W, and C are the same quanities listed above, and θ_2 is the angle between the acceration vector of the spacecraft antenna phase center (shown in figure 18) and the ground station line of sight to the spacecraft. Two-way doppler rate can be calculated by adding the uplink doppler rate and the downlink doppler rate calculated for the two different uplink and downlink frequencies.

In figure 20 the two-way doppler and two-way doppler rate are shown in the range of 30 milli-seconds before the peak of the main lobe and 30 milli-seconds after the peak of the main lobe. Table 7 shows the calculated and measured two-way doppler for various portions of the spacecraft antenna pattern. Also shown is the calculated two-way doppler rate.

TABLE 7. CALCULATED AND MEASURED 2 WAY DOPPLER RESULTS

Position	Calculated 2-Way Doppler (Hz)	Calculated 2-way Doppler Rate (Hz/sec)	Measured* 2-way Doppler (Hz)
#1 (Peak of 1st side lobe)	+32	.476	+31
#2 (-20 db on 1st side of Main Lobe)	-1	535	-3
#3 (Peak of Main Lobe)	-36	448	-31
#4 (-20 db on 2nd side of Main Lobe)	-59	234	-54
#5 (Peak of 2nd side lobe)	-67	19	-72

* The accuracy of the measured values is expected to have a tolerance of ± 5 Hz because of the uncertainty in determining precisely the instantaneous frequency at the ground station.

5.7 Spacecraft Noise Temperature

The spacecraft system noise temperature is dependent upon several factors; primarily the earth noise temperature, noise figure of the transponder and the receive losses of the transponder. The following formula is used to calculate the spacecraft system noise temperature.

$$T_S = T_A + T_T + (LF-1)\, T_o \quad {}^\circ K$$

where T_A is the antenna sky noise, T_T is the noise spillover from the transmitter in the receiver band, L is the losses from the antenna to the front end of the receiver, F is the noise factor of the receiver, and T_o is the actual temperature of the coupling network between the antenna and the receiver. The noise factor is given by the following formula

$$F = (1 + T_R/t_o)$$

where T_R is the receiver effective noise temperature and t_o is 290°K (reference temperature).

The spacecraft repeater has a noise figure of 5.5 db at the input to the electronics. The receive antenna losses were measured prior to launch and are equal to 2.3 db. Based upon ATS-1 data for a similar repeater we would expect the temperature of the coupling network to be about 285°K while 40°K is a reasonable assumption for the degradation due transmitter thermal noise out of band. The antenna sky noise is taken to be 290°K when looking directly at the earth. Using these values in the formula above yields the spacecraft system noise temperature.

$$T_S = T_A + T_T + (LF-1)\ T_o$$

$$= 290°K + 40°K + \left[1.7\ (3.5)\ -1\right]\ 285°K$$

$$= 1760°K \quad 32.5\ db \quad °K$$

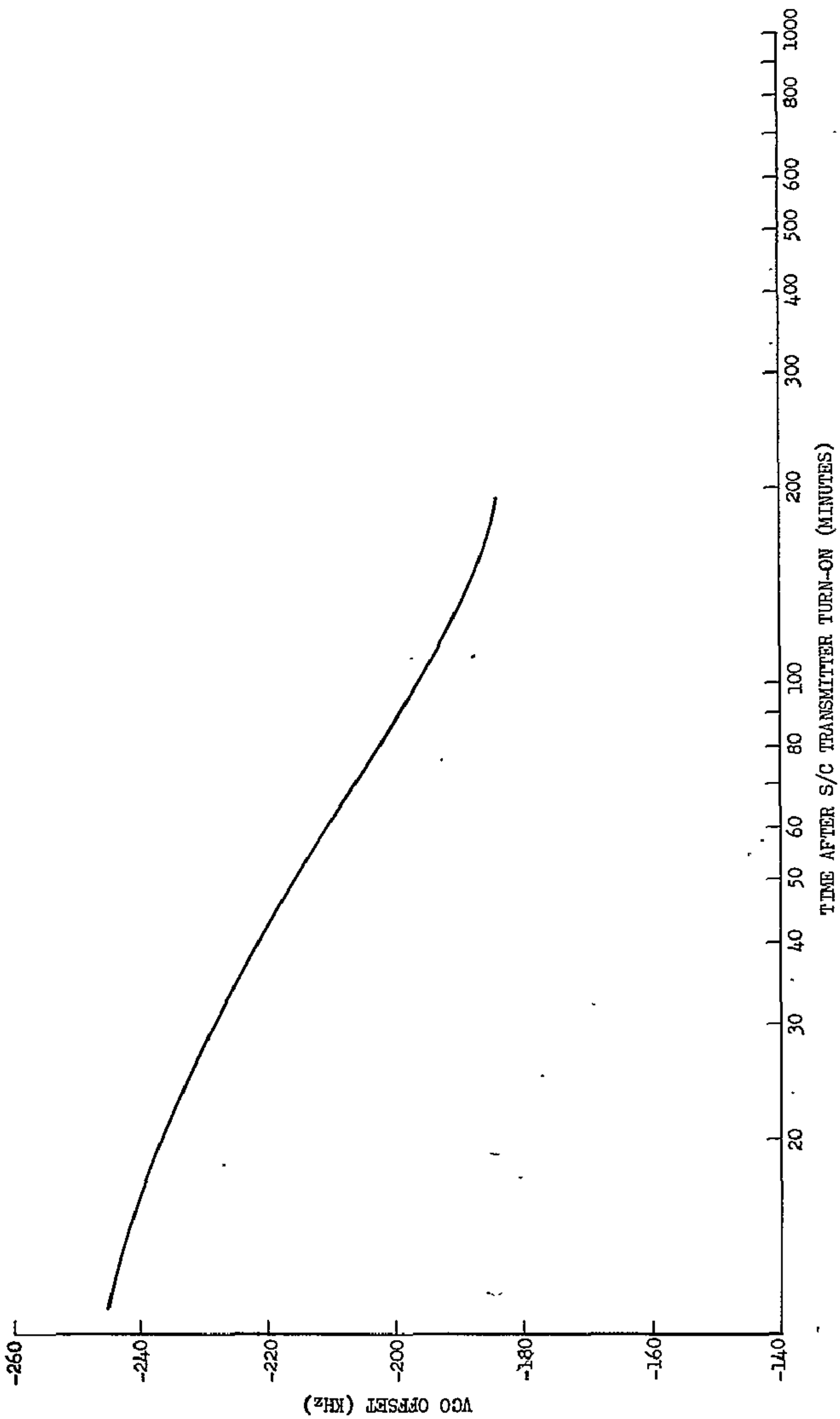

Figure 12. ATS-5 L-Band Frequency VCO Offset and Drift

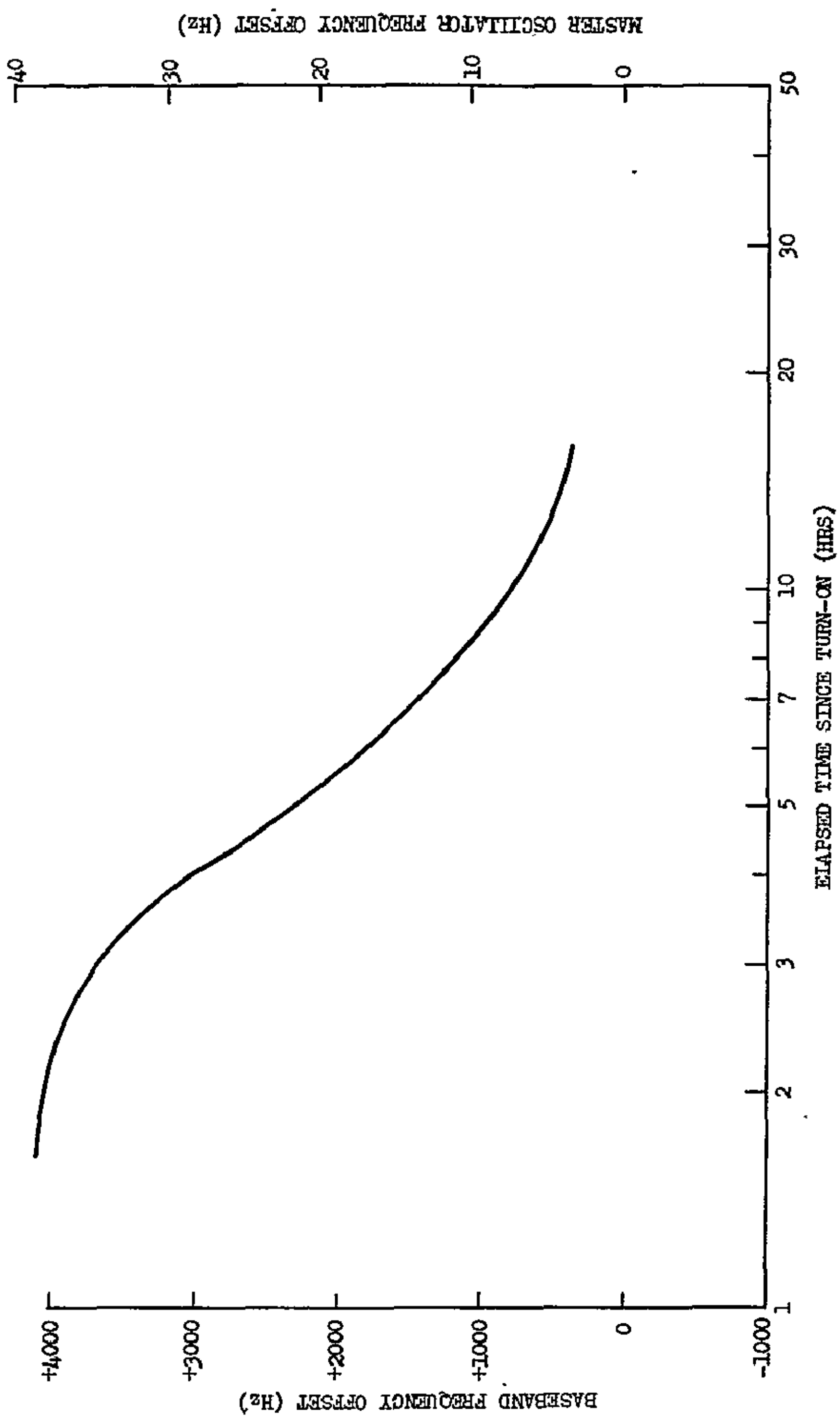

Figure 13. ATS-5 L-Band Master Oscillator Offset

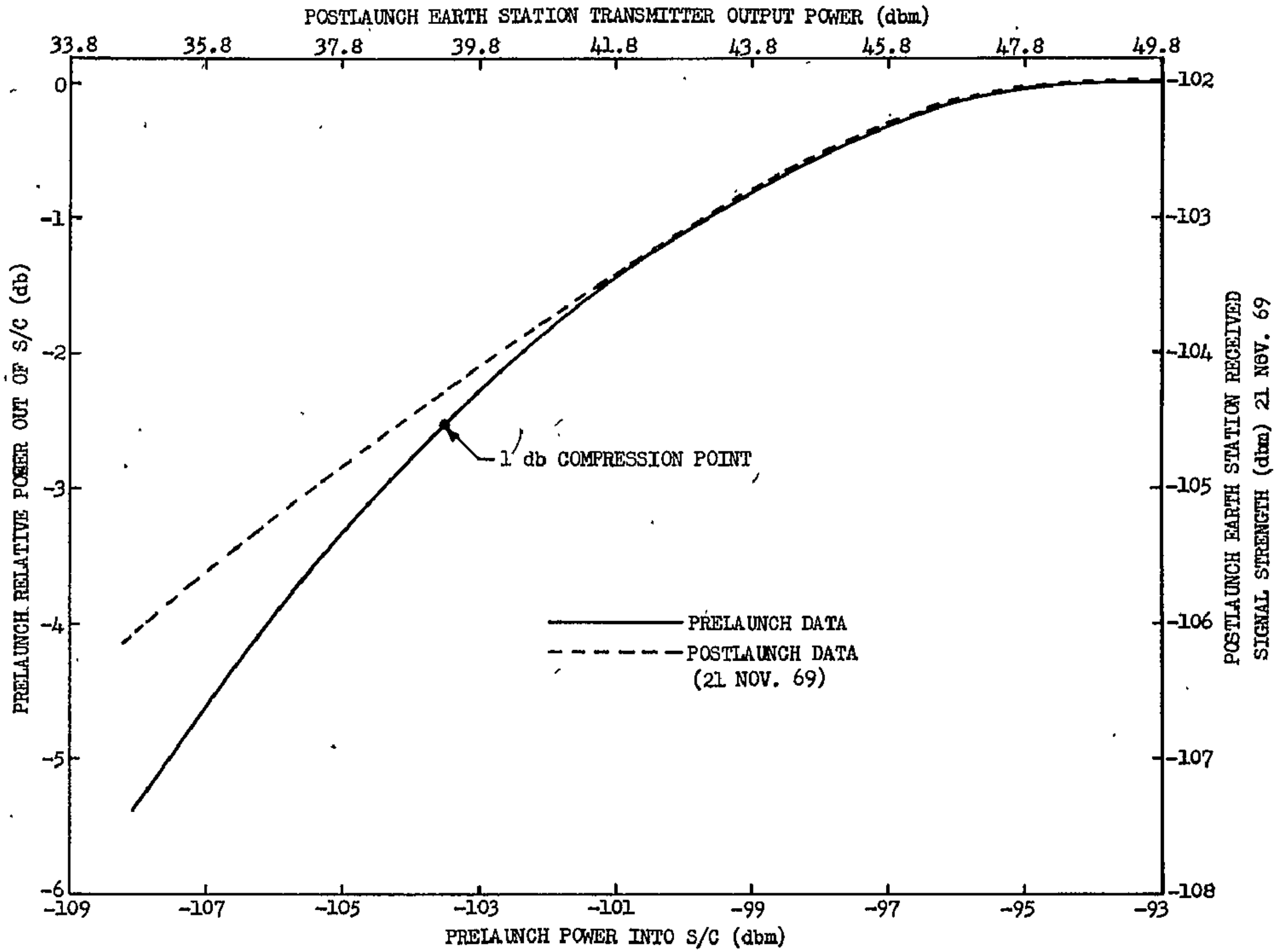

Figure 14. ATS-5 Transponder Input/Output Characteristics (L-L NBFT Mode)

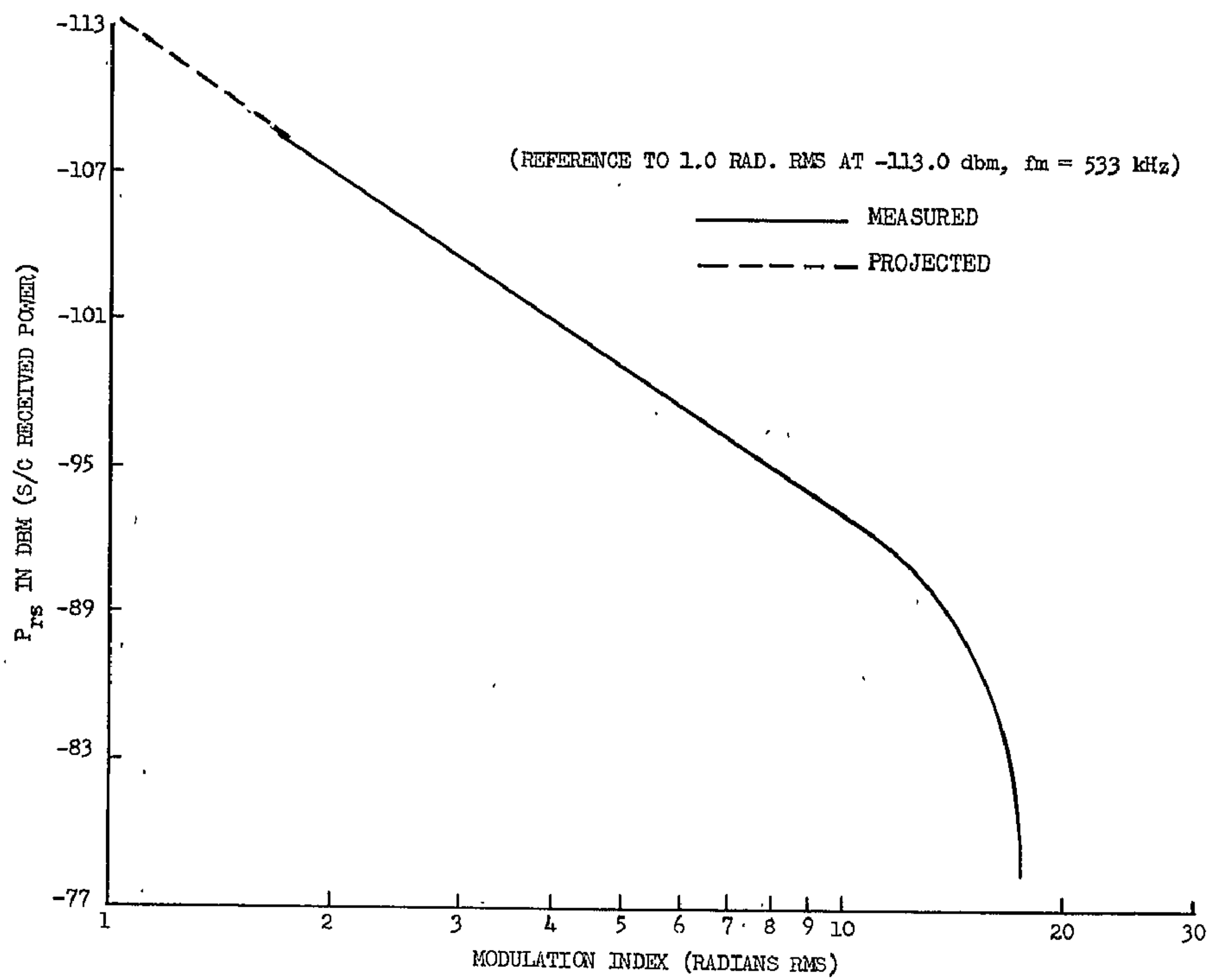

Figure 15. S/C FM Modulator Characteristics

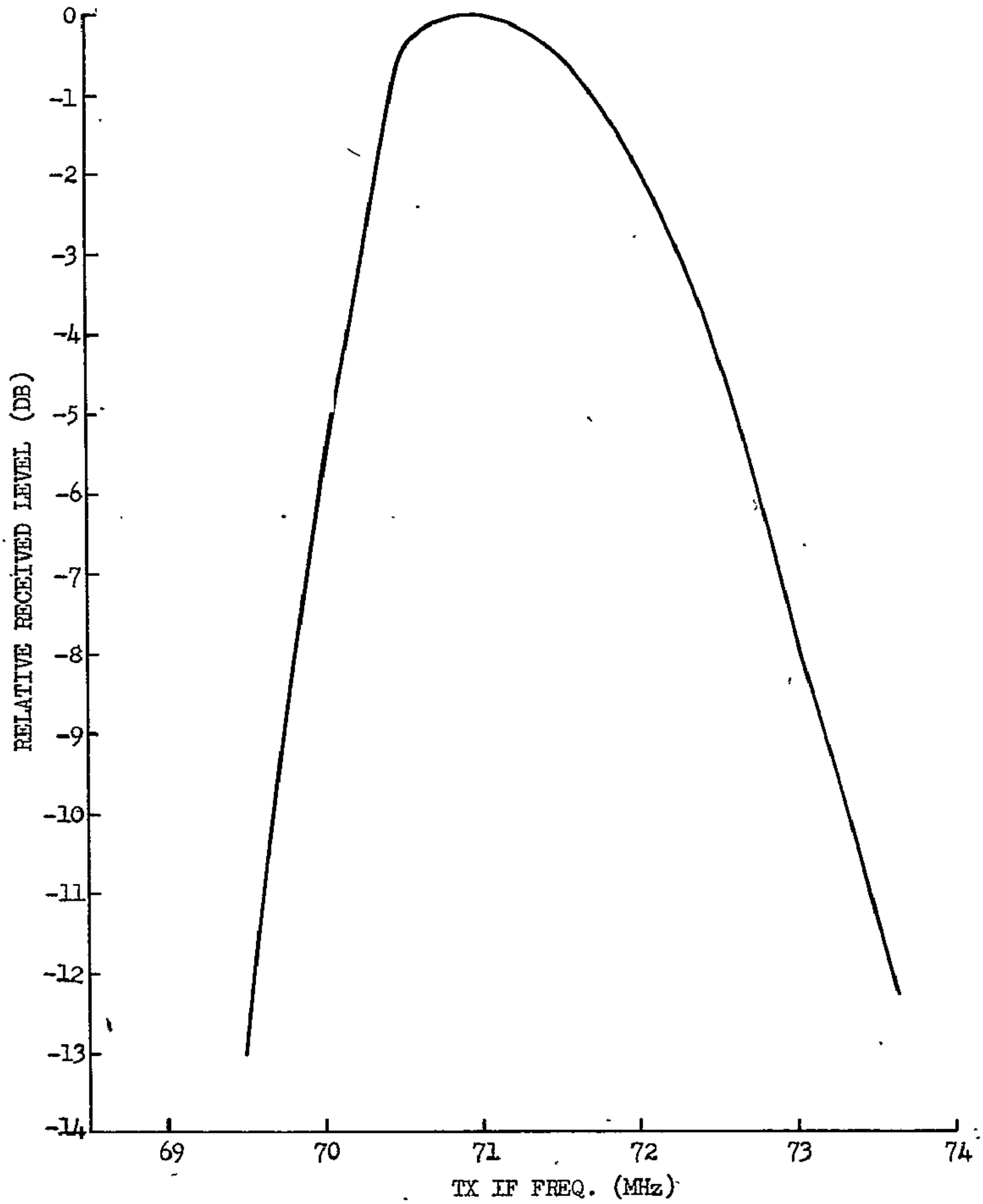

Figure 16. ATS-5 L-Band FTNB Mode Frequency Response (1TWT)12/3/69

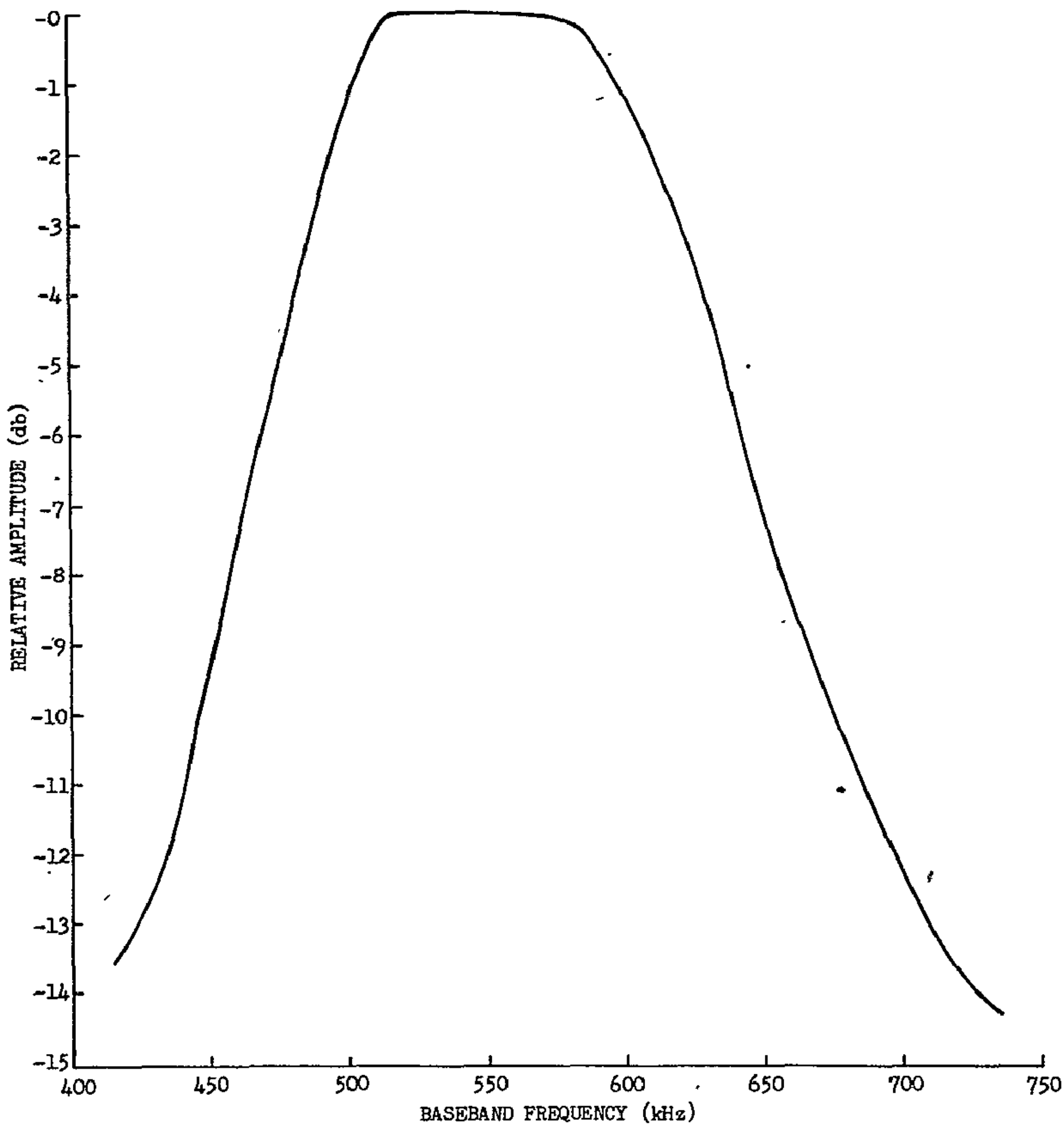

Figure 17. ATS-5 L-Band MA Mode Frequency Response

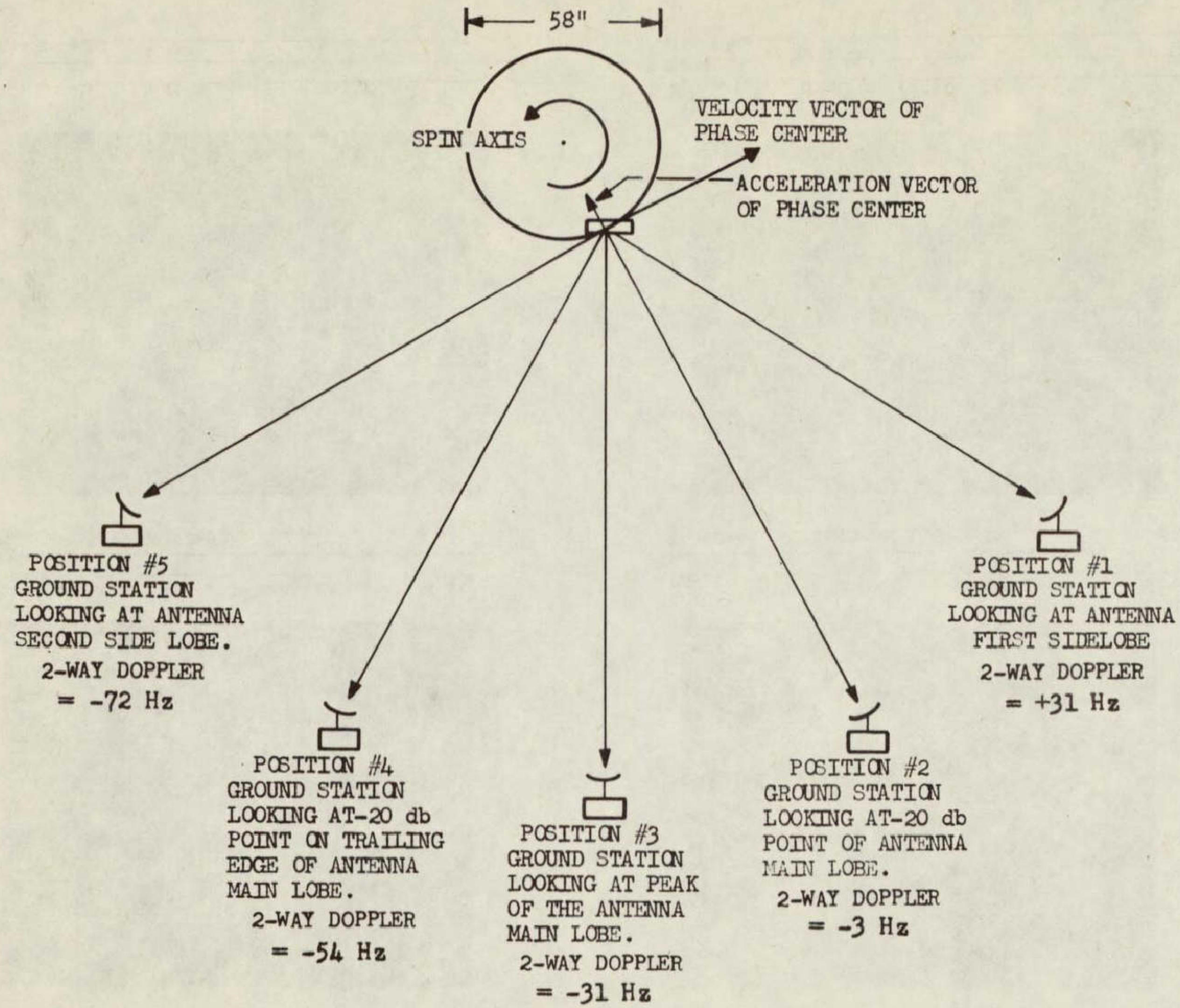

Figure 18, Spacecraft/Earth Station Configuration For Receiving Various Portions of the Antenna Pattern

ATS COMMUNICATIONS TEST

ETP________ Serial No.________ Date________ Flight No.________ Time________

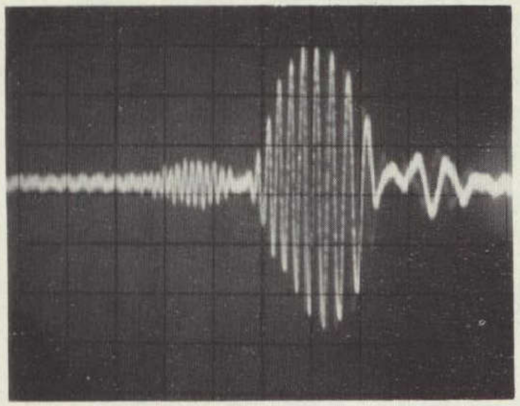

1

Picture Title: Main and side lobes of received signal
Scale:
Time Base: 50 msec/cm

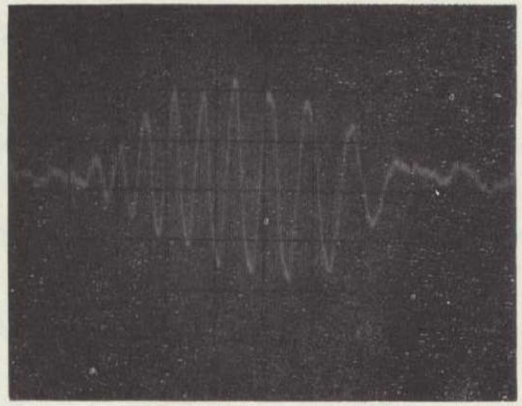

2

Picture Title: Main lobe of Received Signal
Scale:
Time Base: 20 msec/cm

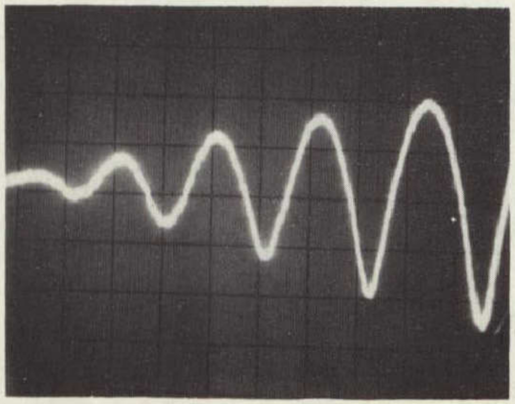

3

Picture Title: Leading edge of main lobe
Scale:
Time Base: 5 msec/cm

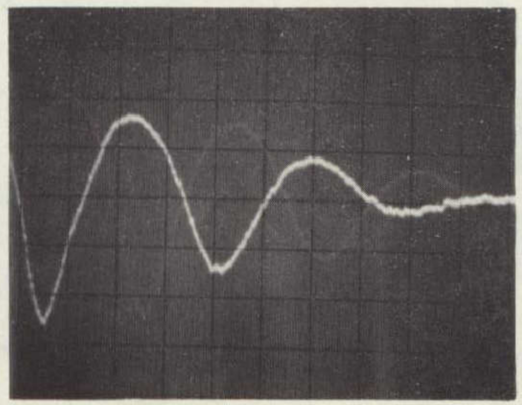

4

Picture Title: Trailing edge of main lobe
Scale:
Time Base: 5 msec/cm

Figure 19. ATS-5 Spin Doppler

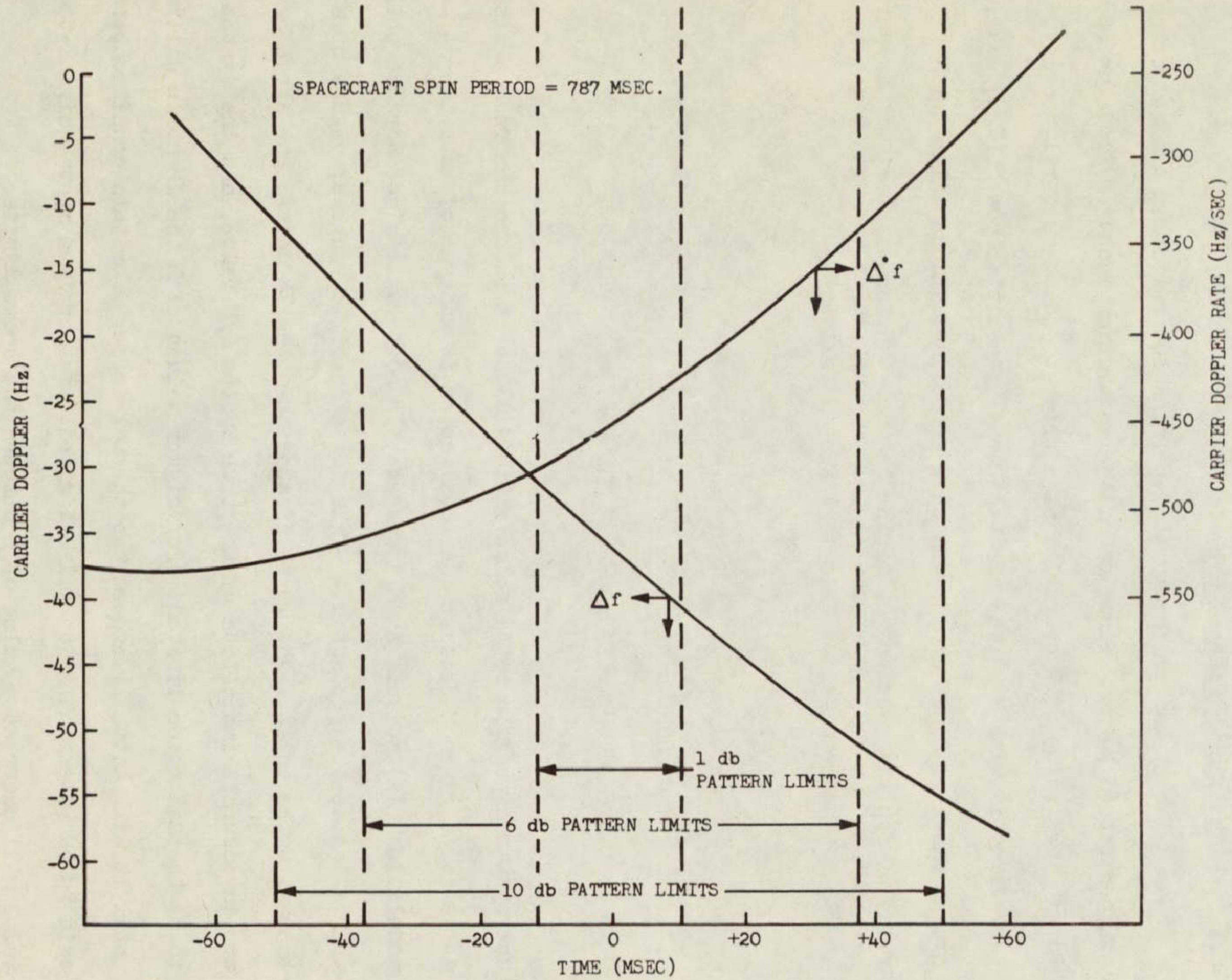

Figure 20. Two Way Doppler Profile

6 SYSTEM PERFORMANCE CHARACTERISTICS

6.1 Multiplex Channel S/N

A test was performed to determine the multiplex channel signal to thermal noise ratio (S/N) as a function of the modulation index (M) for the SSB/FM system. For a given value of a overall link carrier-to-noise spectral density, S/N will vary directly with M^2. The SSB test tone transmitter power (P_{tg}) was varied over a range of 41 dbm to 50 dbm thus producing various values of M. For each value of P_{tg} the received multiplex channel S/N, unweighted, was measured.

The results for this test are as follows:

P_{tg} (dbm)	S/N (db)
41	26
44	30
47	33
50	36

The system signal to total noise ratio will be less than the values listed above for a given M because the total noise is made up of both thermal and intermodulation (IM) noise. As M increases, IM noise will also increase while the thermal noise stays constant. Thus for a specific range of values of M where the thermal noise is at least 10 db greater than the IM noise, the above S/N values are an accurate indication of the true system S/N value, and the system is said to be thermal noise limited. For higher values of M the IM noise will increase until it will actually exceed the thermal noise. For this condition, the system is said to be intermodulation noise limited. The optimum system signal-to-total noise value will occur at a value of M between the above limits.

6.2 Spin Modulation Compensation Test

All signals transmitted from the earth station to the spacecraft will undergo an amplitude change due to the spacecraft antenna gain. The signal enhancement due to the antenna will be a function of the antenna pattern and the relative angle of arrival of the propagated signal. As the spacecraft spins about its axis, the angle between the received signal propagation vector and the antenna boresight changes through 360°. This has the effect of amplitude modulating the received signal with the spacecraft antenna pattern (as received at the electronics input)

The effect of the spin modulation may be overcome by amplitude modulating the transmitted signal with the inverse of the spacecraft antenna pattern. The modulation must be timed so that the modulated signal arrives at the spacecraft with minimum level when the effective antenna gain is greatest, and visa versa.

The extent to which the spin modulation may be overcome is a function of the available power at the earth station and the spacecraft antenna pattern. The SSB transmitter used for the L-band experiments may be operated at an output power of 15 to 20 db greater than that required for good uplink performance (the transmitter power output capability is determined by the FM/FM mode, which is much greater than that required for SSB/FM operation). It is therefore possible to compensate for up to 20 db of the spin modulation, however, in order to stay within the linear portion of the transmitter output characteristic, only up to 15 db of compensation was utilized.

The test was performed by amplitude modulating input to the earth station SSB transmitters by using a pin diode attenuator in the 70 MHz IF.

The modulating signal was provided by the on-site computer via a digital to analog converter.

The computer was programmed to provide an output voltage which was essentially the inverse of the spacecraft antenna pattern (the actual function contained corrections for the pin diode modulation linearity as well as the transmitter linearity). The computer was cycled once each spin revolution of the spacecraft by the timing unit which was synchronized with the spacecraft spin. The propagation delay from the earth station to the spacecraft was compensated for by the timing unit.

The test consists of four basic steps as follows:

1) Synchronization is established between the modulating signal (S_M) (derived from the computer stored program) and the spacecraft. This is best accomplished by simultaneously viewing S_M (D to A output) and the spacecraft transmit antenna pattern on an oscilloscope (frame 1 of figure 21). Both the computer and the oscilloscope are gated from the synchronization and timing (S/T) unit.

2) The 3 db pulse width of S_M is compared with the spacecraft transmit antenna pattern and the computer program is adjusted if necessary, to make the 3 db points approximately the same (frame 3 of figure 21). This step is required because of the nature of the computer program and would not be necessary in an operational system which would use an adaptive technique. The spacecraft transmit antenna pattern is used for the comparison instead of the receiver pattern because of the relative ease with which the former is obtained. The patterns may be considered identical for the purpose of this test.

3) The proper time delay is established between the D/A output (S_M) and the spacecraft transmit antenna pattern. This is accomplished by advancing the gating pulse to the computer by approximately 0.25 sec. (round trip propagation time to the spacecraft). The time advancement is readily performed using the built in digital phase adjustment in the S/T unit.

4) Final alignment of SM is accomplished by observing the spacecraft receive antenna pattern on an oscilloscope and adjusting the time delay for a best "fit" as determined by obtaining a maximum effective beamwidth of the spacecraft receive antenna pattern.

Frame 3 of figure 21 shows the receive antenna pattern without spin modulation compensation (top trace); the bottom trace is a 3 db calibration trace used to calibrate the amplitude of the received signal. Frame 4 shows the receive antenna pattern with the compensation circuits activated (top trace); also shown is a 3 db calibration (bottom trace). The 600 Hz audio frequency ripple component is present in both frames due to the relatively large frequency response of the AM detector.

The effectiveness of the test was determined by measuring the uplink spacecraft antenna pattern with and without the pin diode attenuator modulated. The results showed that the 3 db beamwidth was effectively increased from about 54 ms to 100 ms. The top of the pattern showed ripple of about 0.5 db, however, further refinement of the stored computer function could reduce the ripple even further.

No effort was made to provide adaptive logic to compensate for the spin modulation, however, an adaptive technique could easily be implemented.

7 CONCLUSIONS

Tests performed with the ATS-5 spacecraft have shown that, even though it is spin stabilized, most of the engineering data may be obtained. The spacecraft operational characteristics have been measured, in a space environment, and the test results indicate that the system is functioning normally. Link calculations have been verified with test data and the utilization of a timing and synchronization unit allows accurate measurements to be made through the spacecraft during the time interval that the spacecraft antenna illuminate the earth station.

Propagation tests have been performed which show that diurnal effects and short term fading at L-band are negligable (less than $\pm$ 0.5 db).

The test techniques described herein, together with the measured ATS-5 spacecraft operational characteristics, provide the basic information required in order to proceed with the development of tests to measure multipath effects.

ATS COMMUNICATIONS TEST

ETP________ Serial No.________ Flight No.________ Date________ Time________

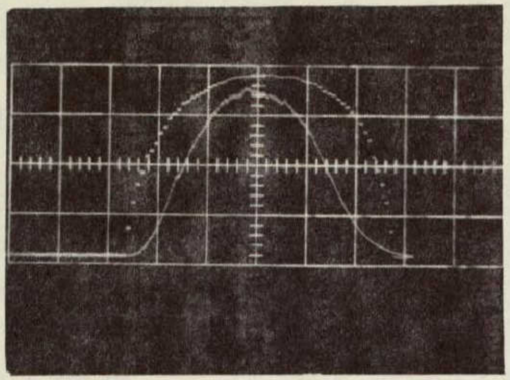

1

Picture Title: Modulating Signal & S/C Transmit Ant. Pattern
Scale: Linear (Top), Log (bottom)
Time Base: 20 ms/cm

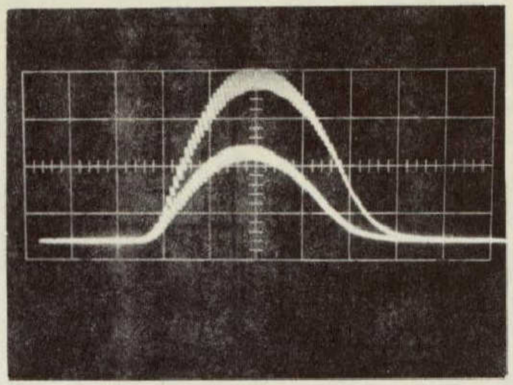

2

Picture Title: Mux Output (uncompensated)
Scale: Linear (with 3 db calibration)
Time Base: 20 ms/cm

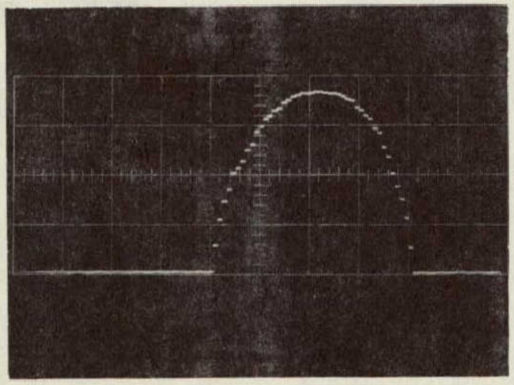

3

Picture Title: SSB Transmitter Modulating Signal
Scale: Linear
Time Base: 20 ms/cm

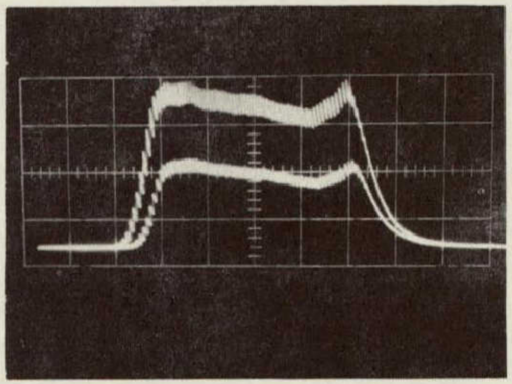

4

Picture Title: Mux Output (Compensated to 15 db)
Scale: Linear (with 3 db calibration)
Time Base: 20 ms/cm

Figure 21. Spin Modulation Compensation Test Waveforms

Appendix A

CONSIDERATION OF PARAMETERS AFFECTING PROPAGATION MEASUREMENTS

A.1 ORBIT GEOMETRY

Figure A.1 shows the orbit geometry of the ATS-5 spacecraft.

The orbit of the spacecraft is inclined approximately 2.5° to the earth's equitorial plane. The axis of spin of the spacecraft is perpendicular to the earth's equitorial plane. The spacecraft spins CCW (looking down from the north), which is the same as the earth's spin direction.

It is important to note that as the spacecraft orbits the earth, its subtrack moves north and south as shown in figure A.2. The impact that this movement has upon off beam center allowance is illustrated in detail in figure A.3.

As the spacecraft moves north and south in its orbit, it is useful to consider what areas of the earth are covered by the 1 and 3 db beamwidths of the spacecraft antenna. Considering a stationary earth, a non-spinning spacecraft and assuming a conical beam, the 1 and 3 db antenna patterns are approximately as shown in figure A.3 for the northern and southern most excursions of the spacecraft. It may be noted that as the spacecraft moves from N to S, a small circle on the earth's surface is always within the 1 db beamwidth. Also, as the spacecraft moves from north to south and back, it is seen that the 3 db beamwidth sweeps across the earth in such a manner that another area of the earth is always within the 3 db beamwidth, and may also be at times within the 1 db beamwidth. Thus, this area (which contains the Mojave ground station), may be anywhere from 0 to 3 db down from the boresight of the antenna (assuming a symmetrical antenna pattern). A third area indicated in the figure represents the area of the earth which is always at least 1 db off the antenna boresight, and may be as much as 3 db. It is of interest to note that no point on the earth that is illuminated by the spacecraft antenna is ever more than 3 db off boresight. As the spacecraft spins about its axis, the antenna beam sweeps across the earth from east to west, causing each of the concentric circles in figure A.3 to become a "bar" across the earth's surface. The "bar" (not shown in the figure) is essentially parallel with the earth's equator.

The foregoing information concerning the spacecraft orbit geometry was derived from the orbital parameters as provided by NASA/GSFC. Additional information concerning the right ascension and declination of the spacecraft spin axis with respect to the earth's equitorial plane is required before accurate predictions of off beam center allowance may be derived for comparison with measured values. Work is currently in progress in this area.

A.2 POLARIZATION LOSS

Figure A.4 shows the interaction of an elliptically polarized waveform with an elliptically polarized antenna. As seen from the left, the E vector of the propagating wave describes an ellipse at any point along its path. Using the interface of the antenna feed as a point of observation, we see that the H vector of the antenna also describes an ellipse, one which will be at some as yet unknown angle with the incident wave. The E vector of the incident waveform and of the antenna are coincident at the point of observation. The H vectors, which are always 90° out of phase with their respective E vectors, are also coincident at the point of observation.

The actual amount of energy transfer between the incident wave and the antenna is represented by the shaded area of the two ellipses. Maximum transfer of energy will occur when the major axis of both ellipses are aligned, however, total energy transfer will not occur even then unless both ellipses are of the same degree of ellipticity. The spacecraft antenna is required to have an ellipticity less than 2.0 db, the earth station antenna has been measured to have an ellipticity of 2.5 db for transmit and 3.0 db for receive. This results in a minimum polarization loss of 0.01 db for the up and down links, and maximum losses of 0.34 db and 0.29 for the uplink and downlink, respectively. The angle of orientation is a function of the electron density in the ionosphere which gives rise to Faraday rotation of the incident waveform.

A.3 OFF BEAM CENTER ALLOWANCE

Accurate prediction of the off beam center allowance is required if other propagation effects (such as atmospheric diurnal variations) are to be observed. An estimate of the off beam center allowance may be made from measured signal strength (at peak of antenna pattern) for antenna patterns made during several 24 hour tests. Since the spacecraft transmitted power was constant, the variation in earth station received power (at the peak of the pattern) is due to the station being off boresight of the spacecraft antenna. Accurate predictions of off beam center allowance make it possible to detect other losses such as diurnal effects, which are of lesser magnitude. An analysis for the downlink results in an estimated off beam center variation of 2.0 db from the max north to max south excursion of the spacecraft.

Figure 11 shows this predicted variation for Mojave, California on 30/31 January 1970. The peak-to-peak amplitude of the variations, and the phase, will vary according to the location of the measuring station. There is also a phase shift of 360° over a period of one year for any fixed station on the earth.

As discussed previously, the off beam center allowance is a function of the orbit geometry and the spacecraft antenna pattern. During its orbital period, the spacecraft antenna boresight moves north and south a distance which is proportional to:

$$R(\tan \theta + \cos \phi \sin B)$$

where:

R = a time variant function which is dependent upon the range of the spacecraft from the center of the earth and the subsatellite point.

θ = inclination angle of the spacecraft orbital plane with respect to the earth's equitorial plane.

ϕ = declination of the spacecraft spin axis with respect to the earth's equitorial plane.

B = angle in the earth's equitorial plane between the projection of the antenna boresight and the projection of spacecraft spin axis.

From the foregoing, it may be seen that the accuracy of prediction of spacecraft off beam center allowance is dependent upon the accuracy to which the orbital elements are known as well as the accuracy of the antenna pattern model. Data has been taken (figure 11) at Mojave which indicates that the spread between maximum and minimum off beam center allowance is 2.6 db for the downlink. The uplink spread is expected to be identical although this has not been verified. Assuming a conical antenna pattern, it may reasonably be estimated that when the Mojave station is closest to spacecraft antenna boresight, it is still about 0.3 db from the actual spacecraft antenna pattern peak. Thus, the off beam center allowance for maximum north and south spacecraft excursions is assumed to be 0.3 db and 2.3 db for the uplink and the downlink.

A.4 MEASUREMENT TECHNIQUES

The uplink signal strength received at the spacecraft preamplifier input (P_{rs}) is required in order to determine the uplink path loss. In the MA (SSB/FM) mode, P_{rs} is determined from the spacecraft SSB/FM modulator sensitivity and the downlink modulation index. The downlink modulation index is readily determined from the downlink IF frequency spectrum and the spacecraft modulator sensitivity is determined from the spacecraft design specification to be -113.0 dbm ± 2.5 db at the spacecraft preamp input for 1.0 rad. rms modulation index.

If the spacecraft were not spinning, it would be possible to determine P_{rs} in the FT mode by the telemetry readout from the on board P_{rs} sensors, however, the response of the sensors is not fast enough to follow the fluctuation in P_{rs} caused by the spacecraft spin. It is therefore necessary to estimate the value of P_{rs} by comparing pre and post launch spacecraft repeater compression data.

The spacecraft transmitter power output was measured for one and two TWT's during prelaunch tests. The values measured at that time will be used to determine propagation loss.

Accurate measurements of signals, originating at the ATS-5 spacecraft, are complicated by the spacecraft spin. This problem has been overcome by utilizing a synchronized timing unit which provides gating signals to a sample and hold type detector, as well as providing gating signals to other test equipment. As an example, to measure the downlink signal power, the spacecraft is placed in the Wide Band Data Mode (WBDM) which provides an unmodulated downlink carrier at L-band. At the earth station the downlink carrier in hetrodyned to a 70 MHz IF which is divided into two branches. One branch is AM detected and displayed on an oscilloscope (the oscilloscope is gated by the synchronized timing unit). The other branch of the IF is used to provide an input to the sample and hold meter.

The sample/hold detector provides a dc output which is proportional to the RMS of the input signal. The dc output level is maintained by the unit until it is reset by the time synchronization unit. During this "hold" period, the dc output is measured with a digital voltmeter/printer as well as recorded on a strip chart.

By using this technique, it is possible to obtain a measurement of the received signal strength for each revolution of the spacecraft (approximately one reading each 790 ms). It should be noted that as long as the sample time is synchronized with the "flat" portion of the spacecraft antenna pattern, the measured signal will be identical to what would have been measured if the spacecraft were not spinning.

Figure A-5 shows oscillographs of the synchronizer output pulse ("A"), the sample and hold detector output, and the detected IF. The gating pulse "A" and the sample/hold detector output are shown for two time bases (10 and 100 mc/cm). The 100 ms/cm time base shows slightly more than one complete cycle of operation (approximately 1 second total time). A second oscillograph (10 ms/cm) shows the "A" pulse and the sample/hold detector output expanded during the sample interval. Two other oscillographs show the sample/hold detector output in relationship to the detected IF. It may be readily observed that the sample interval is within the "flat" portion of the spacecraft antenna pattern is evidenced by the fact that the detected IF signal is essentially "flat" during this time.

When measuring the downlink antenna pattern, it is convenient to record the detected 70 MHz IF signal on a high speed strip chart recorder (visicorder). This also provides an alternate method of measuring the received signal strength.

A.5 EARTH STATION ANTENNA POINTING

The earth station L-band antenna has no provision for automatic tracking of the spacecraft, however, manual tracking is achieved by updating the L-band antenna pointing coordinates to agree with the C-band antenna which is tracking the spacecraft. The C-band antenna has a half power beamwidth (at the receive frequency) of about 0.4° under normal operational conditions. Since the L-band antenna position (1db beamwidth of approximately 1.7°) is updated before each test, the pointing accuracy will be almost entirely a function of the change in orbit geometry during the test interval, and of the accuracy of the servo drive. The combined effect of these errors is estimated to be 0.5 db $\pm$0.5 db.

A.6 EARTH STATION NOISE TEMPERATURE

The system noise temperature of the earth station is primarily dependent upon the receive antenna noise temperature, T_A; the effective noise temperature of the receiver, T_R; and the receive losses between the antenna and the receiver, L. The formula utilized for calculation of system noise temperature, T_S, is

$$T_S = T_A + T_T + \left[L \left(1 + T_R/t_o\right) - 1 \right] T_o$$

where T_A equals 55°K, T_T is negligible, L equals 1.0 db, T_R equals 170°K, t_o is a reference temperature equal to 290°K, and T_o is the actual temperature of the coupling network equal to 290°K. Using these values the system noise is calculated to be 334°K or 25.3 db °K.

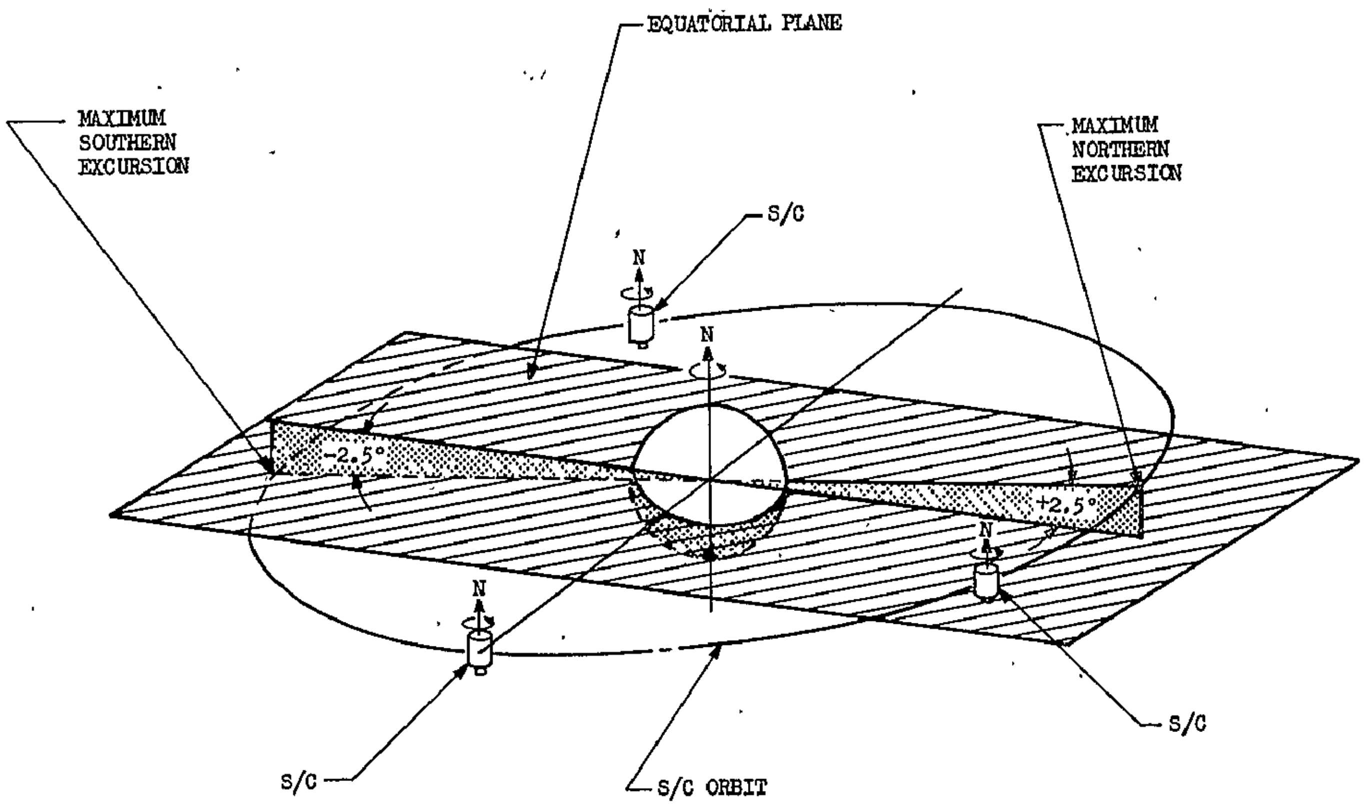

Figure A-1. ATS-5 Orbit Geometry (13 November 1969)

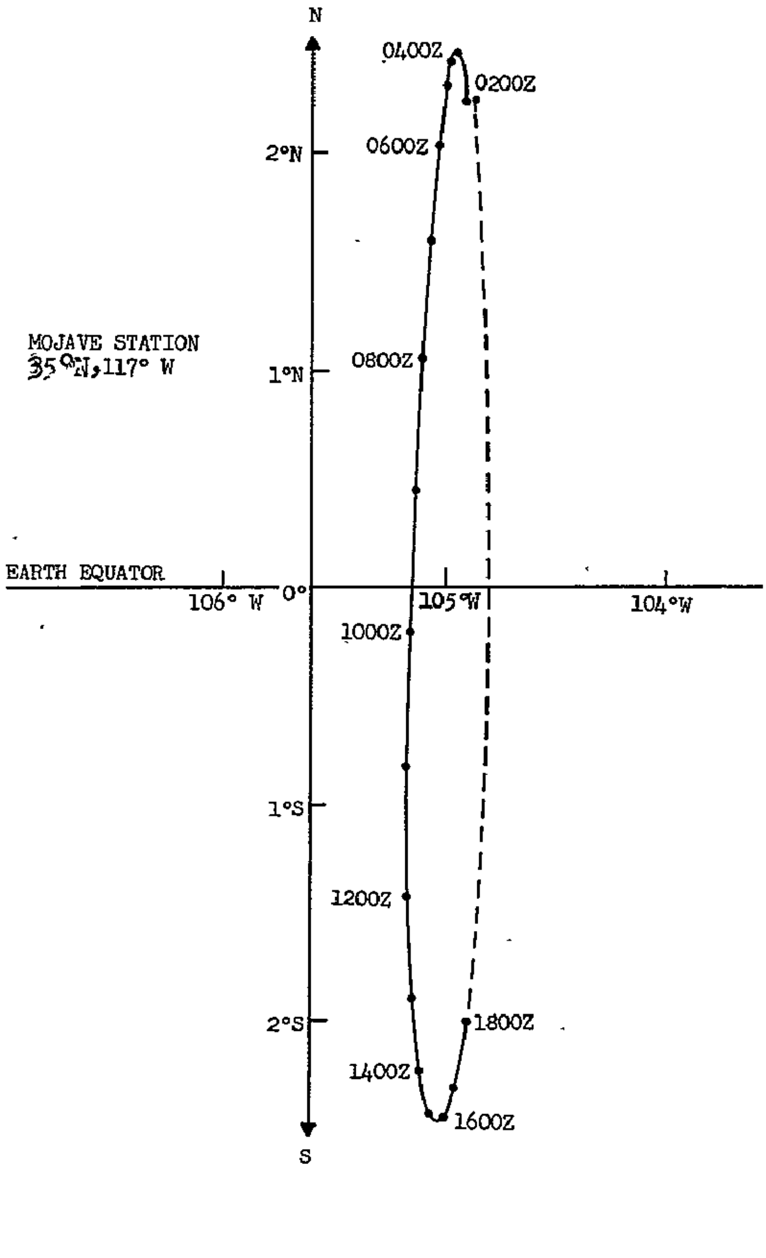

Figure A-2. Sub-track of ATS-5 Spacecraft (13 November 1969)

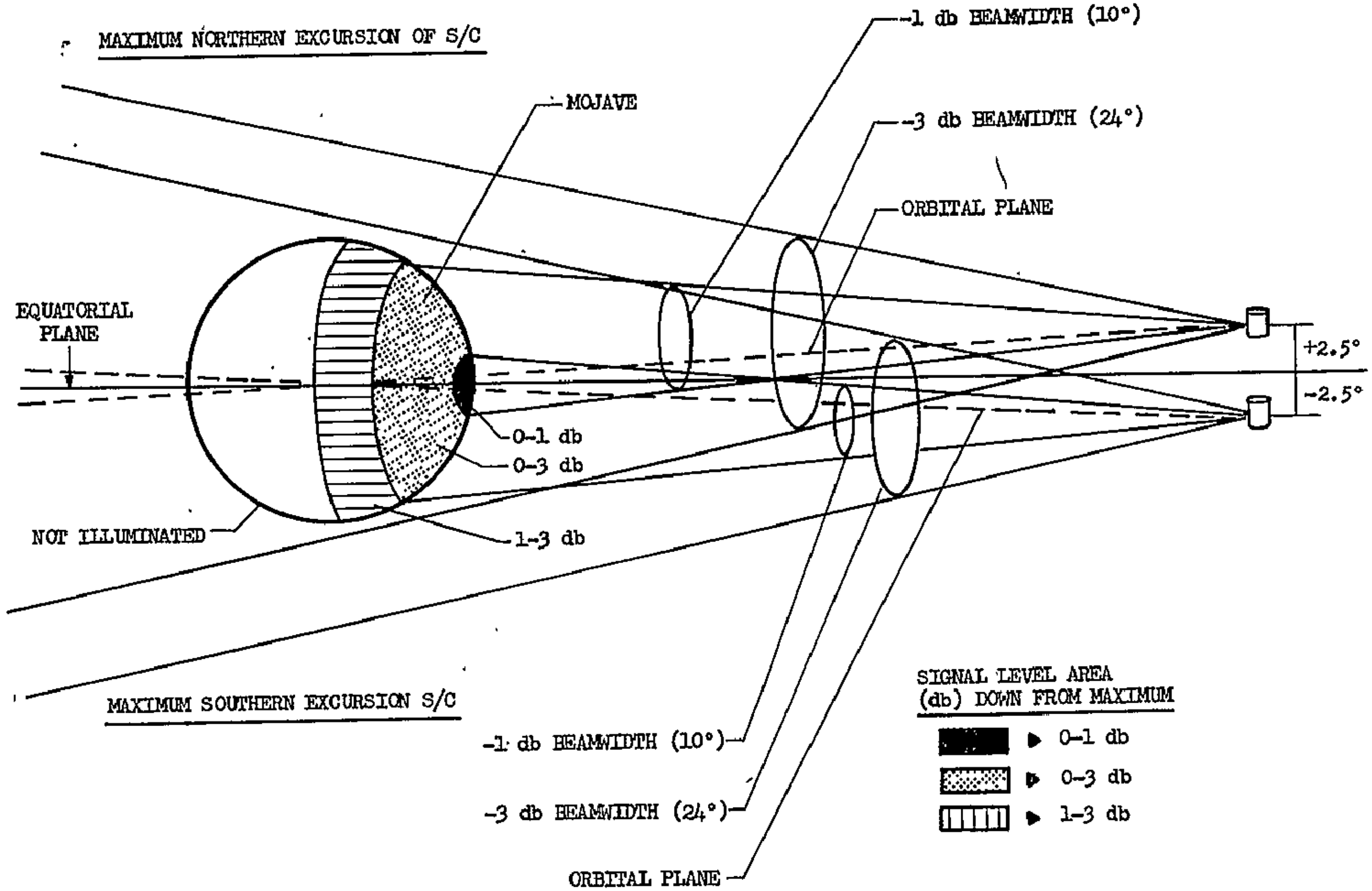

Figure A-3. ATS-5 Earth Illumination/Intensity (13 November 1969)

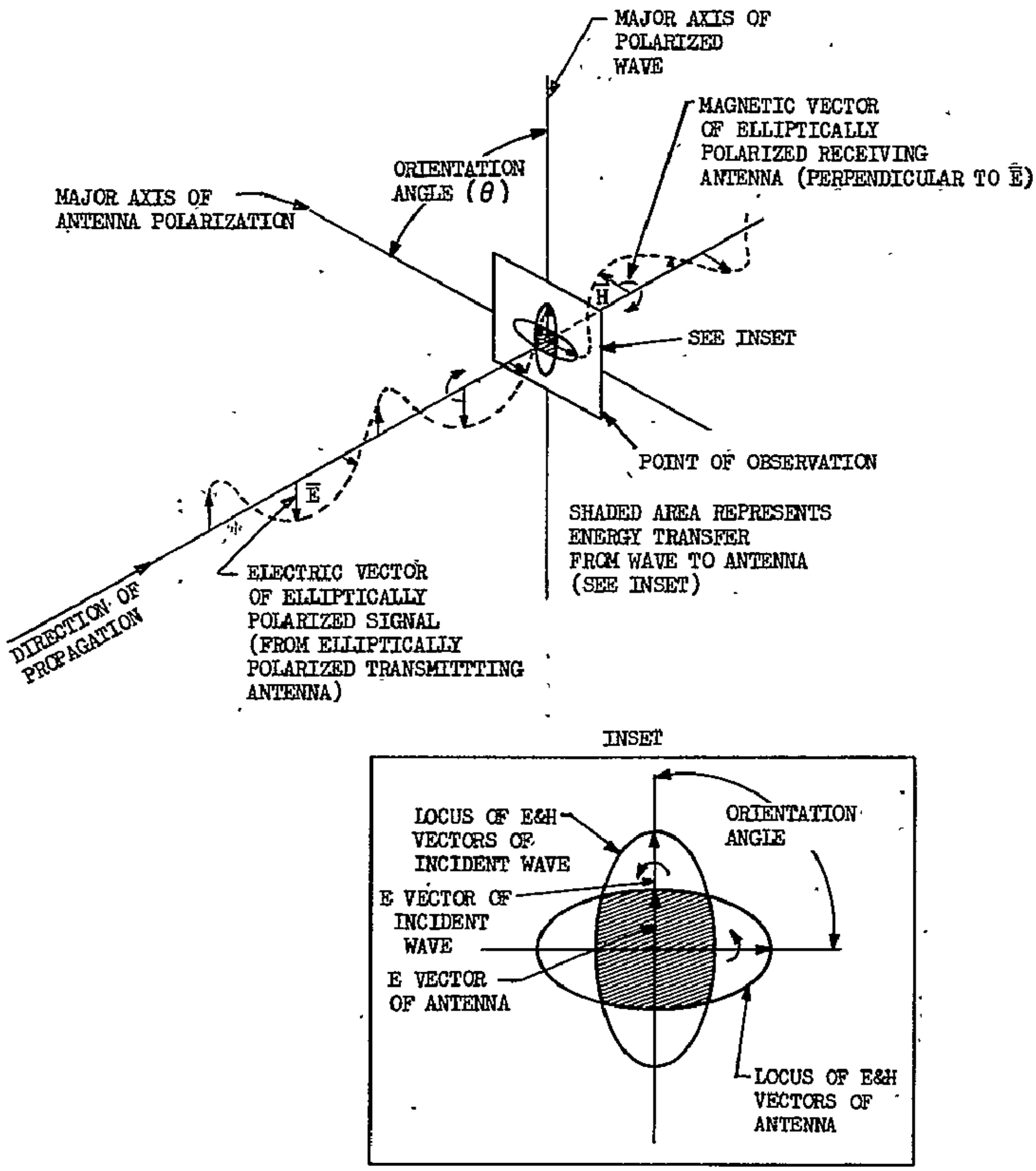

Figure A-4. Energy Transfer Between Elliptically Polarized Antenna

ATS COMMUNICATIONS TEST

ETP L-Band Propagations Serial No. ATS-5 Date 1/25/70 Flight No. ______ Time ______

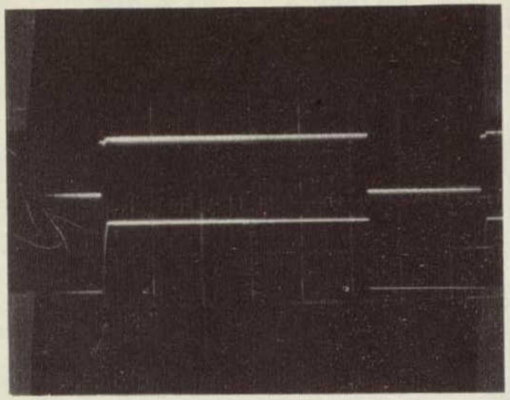

Picture Title: Sample & Hold METER ("A & OUTPUT)
Scale: 5v/cm
Time Base: 100 ms/cm

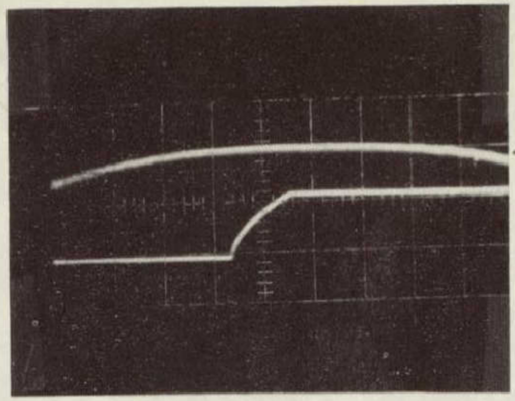

Picture Title: S&H Meter Operation (Detected IF & Output)
Scale: 10 db/cm (top) 5v/cm (bottom)
Time Base: 10 ms/cm

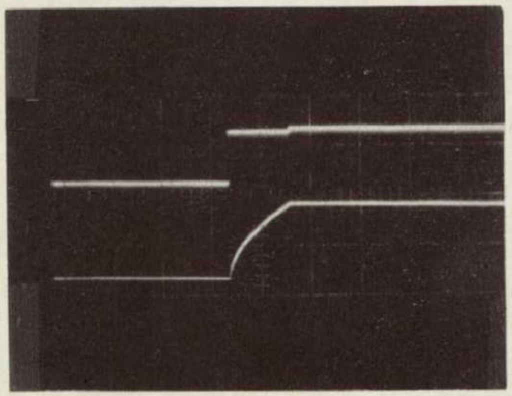

Picture Title: S&H Meter (A pulse & output)
Scale: 5v/cm
Time Base: 10 ms/cm

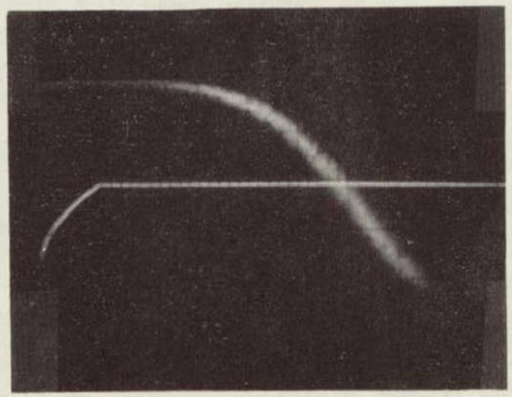

Picture Title: S&H Meter Operation (Detected IF & Output)
Scale: 5 db/cm Top 5v/cm bottom
Time Base: 10 ms/cm

Figure A-5. L-Band Propagation Timing and Synchronization

Appendix B

RANGE AND RANGE RATE TEST RESULTS

This appendix presents the results of a three week study program performed by the Electronics Division of General Dynamics, San Diego Operations, for NASA/GSFC under Contract NAS 5-20128.

OBJECTIVES

The study performed concerned the use of the Applications Technology Satellite Range and Range Rate (ATSR) System with spinning spacecraft. The objective of the study was to determine a feasible and economical modification to the ATSR System which, when implemented, will allow the system to reliably obtain range and range rate data from a spinning spacecraft whose antenna is rotating (front-to-back) such that it is transponding only intermittently. An exemplary tracking condition is that provided by ATS-5 operating at L-Band. The modification recommended as a result of the study was to have the following characteristics and provide the ATSR System with the following additional capabilities:

a. The system shall acquire and track a geostationary spacecraft which is amplitude modulating the transponded signal as a result of spacecraft antenna spin. In particular, and as a typical example, the system shall track the signal transponded by the ATS-5 spacecraft operating at L-Band and C-Band and by the ATS-3 Spacecraft operating at C-Band.

b. Manual acquisition and range ambiguity resolution is acceptable. After acquisition, however, tracking shall be automatic.

c. The modification shall in no way degrade or remove any of the existing system capability or reliability.

d. Once the modification is installed, the system shall be capable of being configured for the newly provided mode of operation in about 10 minutes.

Reconversion to the original configuration shall also be accomplished in about 10 minutes. Conversion or reconfiguration shall preferably be accomplished by switches, plug-in modules, and/or patch cables.

RESULTS

A recommended modification compliant with all the requirements described above was determined. The modification approach consists primarily of properly adapting the carrier and sidetone phase-locked loop parameters to best suit the received signal characteristics. The adjusted phase-locked loop parameters include order, bandwidth, and to a lesser extent, damping. For range ambiguity resolution, the recommended modification includes circuitry for processing range tone phase errors with a sufficiently long time constant to average several bursts of received signal.

A particularly noteworthy and desirable feature of the recommended modification is that no forced or controlled gating is required in any part of the system. The approach includes no externally controlled sampling or signal processing which must be synchronized to the rotation of the spacecraft. Both range and range rate data sampling is unrestricted and can be performed in exactly the same manner as in the existing system. Therefore, computer data processing may also remain unchanged.

The Mojave ATS station L-Band transmitter used with the ATS-5 Spacecraft has bandwidth limitations which prevent use of the 5-MHz sidetone employed in ATSR Modes 1 and 2. The entire investigation and the recommended modification is, therefore, based on the use of ATSR Mode 3 which employs 500 KHz as the maximum sidetone frequency. The results of the investigation and the selected approach are equally applicable to all ATSR modes but, for economic reasons, the recommended modification provides pulsed mode operation capability for

Mode 3 only. This mode uses 500 KHz as the maximum sidetone frequency. The carrier and sidetone tracking loops were temporarily modified to provide the fundamental and essential elements of the modification approach. The carrier tracking loop was operated as follows:

a. Bandwidth selection switch set to narrow position. Of the three available positions, this position gives the lowest DC gain and longest time constants within the loop filter.

b. Loop transfer function modified to first order. This reduces the frequency error accumulated during the period of no signal.

c. Receiver gain control set to manual and gain increased above normal to widen loop bandwidth. This gives the bandwidth required for rapid acquisition and tracking of carrier phase dynamics.

The sidetone tracking loop was operated with a reduced bandwidth using the narrowband VCXO. No attempt was made to resolve range ambiguities. The system was locked and range and range rate data recorded in the normal manner. Subsequent analysis of the data indicated the following:

a. All samples of range and range rate data were valid.

b. Range rate noise errors ($\sigma_{\dot{R}}$) computed on the basis of 32 samples were generally better than 1 meter per second at a data sampling rate of 2/second and better than 0.2 meters per second at a data sampling rate of 6/minute. A typical set of 32 range rate data samples is shown in Figure B-1.

c. Range rate mean values computed on the basis of 32 samples agreed with range rate mean values computed from prediction data furnished to the site to within 0.5 meters per second in all cases.

d. Range noise errors (σ_R) computed on the basis of 32 samples were less than 0.7 meters. All raw data samples differed from the expected mean by less than one range quantizing increment. A typical set of 32 range data samples is shown in Figure B-2.

e. The rate of change in range data agreed with prediction data to within 0.2 meters per second.

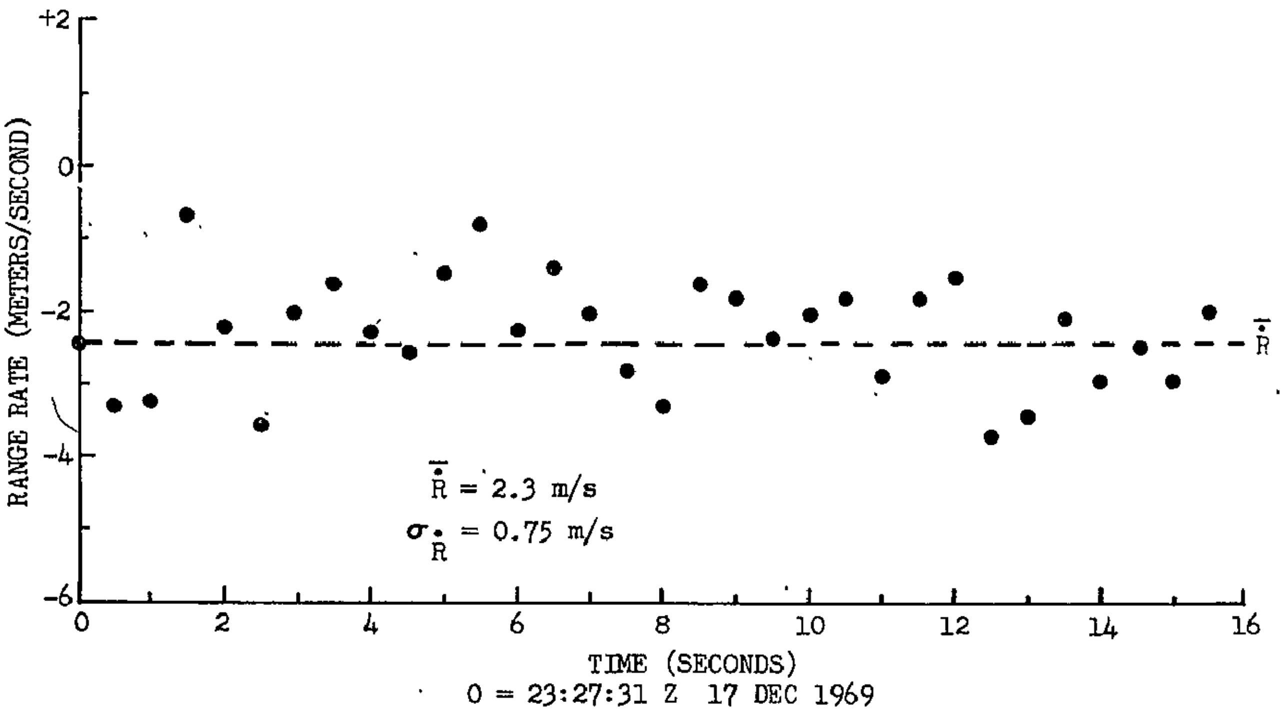

Figure B-1. Typical ATS-5 L-Band Test Range Rate Data

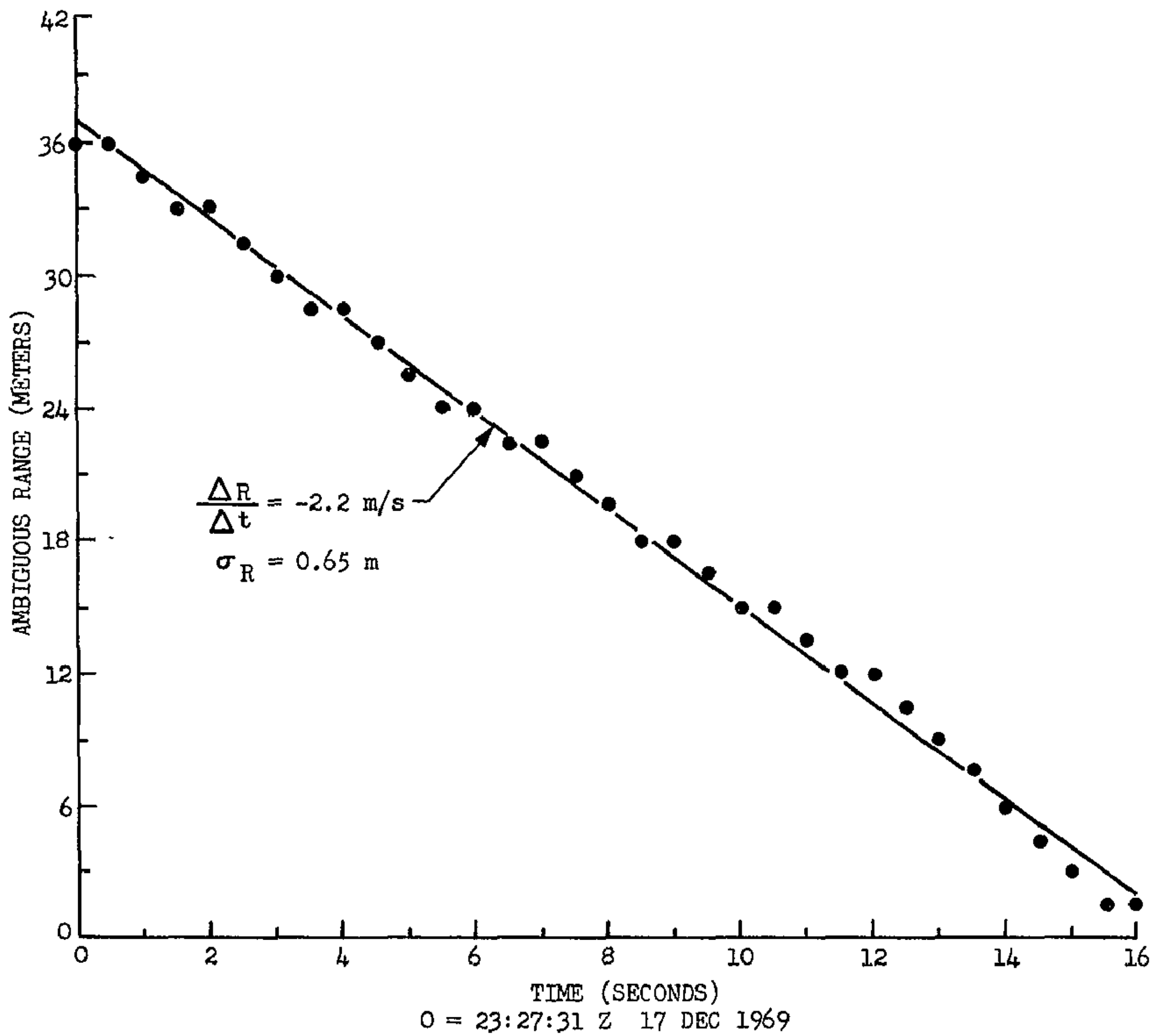

Figure B-2. Typical ATS-5 L-Band Test Range Data